retinoic acid modulation of drug-metabolizing enzyme activities: investigation with selective metabolic drug probes. Cancer Chemother. Pharmacol., *41:* 133–139, 1998.

12. Meyskens, F. L., Jr., Jakobson, J., Nguyen, B., Weiss, G. R., Gandara, D. R., and MacDonald, J. S. Phase II trial of oral b-all *trans*-retinoic acid in hepatocellular carcinoma (SWOG 9157). Invest. New Drugs, *16:* 171–173, 1998.

13. Xu, X. C., Sozzi, G., Lee, J. S., Lee, J. J., Pastorino, U., Pilotti, S., Kurie, J. M., Hong, W. K., and Lotan, R. Suppression of retinoic acid receptor β in non-small-cell lung cancer *in vivo*: implications for lung cancer development. J. Natl. Cancer Inst. (Bethesda), *7:* 624–629, 1997.

14. Sun, S. Y., Yue, P., Dawson, M. I., Shroot, B., Michel, S., Lamph, W. W., Heyman, R. A., Teng, M., Chandraratna, R. A. S., Shudo, K., Hong, W. K., and Lotan, R. Differential effects of synthetic nuclear retinoid receptor-selective retinoids on the growth of human non-small cell lung carcinoma cells. Cancer Res., *57:* 4931–4939, 1997.

15. Matsushima-Nishiwaki, R., Shidoji, Y., Nishiwaki, S., Yamada, T., Moriwaki, H., and Muto, Y. Aberrant metabolism of retinoid X receptor proteins in human hepatocellular carcinoma. Mol. Cell. Endocrinol., *121:* 179–190, 1996.

16. Adachi, S., Okuno, M., Matsushima-Nishiwaki, R., Takano, Y., Kojima, S., Friedman, S., Moriwaki, H., and Okano, Y. Phosphorylation of retinoic X receptor suppresses its ubiquitination in human hepatocellular carcinoma. Hepatology, *35:* 332–340, 2002.

17. Murakami, K., Matsuura, T., Hasumura, S., Nagamori, S., Yamada, Y., and Saiki, I. Involvement of insulin-like growth factor binding protein-3 in the retinoic acid receptor-α-mediated inhibition of hepatocellular carcinoma cell proliferation. Cancer Lett., *151:* 63–70, 2000.

18. Murakami, K., Matsuura, T., Sano, M., Hashimoto, A., Yonekura, K., Sakukawa, R., Yamada, Y., and Saiki, I. 4-[3,5-Bis(trimethylsilyl)benzamido]benzoic acid (TAC-101) inhibits the intrahepatic spread of hepatocellular carcinoma and prolongs the life-span of tumor-bearing animals. Clin. Exp. Metastasis, *16:* 633–643, 1998.

19. Towbin, H., Staehelin, T., and Gordon, J. Electrophoretic transfer of proteins from polyacrylamide gels to nitrocellulose sheets: procedure and some applications. Proc. Natl. Acad. Sci. USA, *76:* 4350–4354, 1979.

20. International Union Against Cancer. Liver. *In:* L. H. Sobin and C. Wittenkind (eds.), TNM Classification of Malignant Tumours, 5th ed., pp. 74–77. New York: Wiley-Liss, 1997.

21. Sever, C. E., and Locker, J. Expression of retinoic acid and receptor genes in liver and hepatocellular carcinoma. Mol. Carcinog., *4:* 138–144, 1991.

22. David, J. M., Umezono, K., and Evans, R. M. The retinoic acid receptors. *In:* M. B. Sporn, A. B. Roberts, and D. S. Goodman (eds.), The Retinoids: Biology, Chemistry, and Medicine, 2nd ed., pp. 319–349. New York: Raven Press, 1994.

23. Hashimoto, Y., Kagechika, H., Kawachi, E., Fukasawa, H., Saito, G., and Shudo, K. Evaluation of differentiation-inducing activity of retinoids on human leukemia cell lines HL-60 and NB4. Biol. Pharm. Bull., *19:* 1322–1328, 1996.

24. Zhang, L. X., Mills, K. J., Dawson, M. I., Collins, S. J., and Jetten, A. M. Evidence for the involvement of retinoic acid receptor RAR α-dependent signaling pathway in the induction of tissue transglutaminase and apoptosis by retinoids. J. Biol. Chem., *270:* 6022–6029, 1995.

25. Pollard, M., and Luckert, P. H. The inhibitory effect of 4-hydroxyphenyl retinamide (4-HPR) on metastasis of prostate adenocarcinoma-III cells in Lobund-Wistar rats. Cancer Lett., *59:* 159–163, 1991.

26. Oikawa, T., Okayasu, I., Ashino, H., Morita, I., Murota, S., and Shudo, K. Three novel synthetic retinoids, Re80, Am580, Am80, all exhibit anti-angiogenic activity *in vivo*. Eur. J. Pharmacol., *249:* 113–116, 1993.

27. Lu, X. P., Fanjui, A., Picard, N., Pfahl, M., Rungta, D., Nared-Hood, K., Carter, B., Piedrafita, J., Tang, S., Fabbrizio, E., and Pfahl, M. Novel retinoid-related molecules as apoptosis inducers and effective inhibitors of human lung cancer cells *in vivo*. Nat. Med., *3:* 686–690, 1997.

28. Murakami, K., Wierzba, K., Sano, M., Shibata, J., Yonekura, K., Hashimoto, A., Sato, K., and Yamada, Y. TAC-101, a benzoic acid derivative, inhibits liver metastasis of human gastrointestinal cancer and prolongs the life-span. Clin. Exp. Metastasis, *16:* 323–331, 1998.

29. Murakami, K., Yamaura, T., Suda, K., Ohie, S., Shibata, J., Toko, T., Yamada, Y., and Saiki, I. TAC-101 (4-[3,5-bis(trimethylsilyl)benzamido]benzoic acid) inhibits spontaneous mediastinal lymph node metastasis produced by orthotopic implantation of Lewis lung carcinoma. Jpn. J. Cancer Res., *90:* 1254–1261, 1999.

30. Angel, P., and Karin, M. The role of Jun, Fos, and the AP-1 complex in cell-proliferation and transformation. Biochim. Biophys. Acta, *1072:* 129–157, 1991.

31. Li, J. J., Dong, Z., Dawson, M. I., and Colburn, N. H. Inhibition of tumor promoter-induced transformation by retinoids that transrepress AP-1 without transactivation retinoic acid response element. Cancer Res., *56:* 483–489, 1996.

32. Hui, A. M., and Makuuchi, M. Molecular basis of multistep hepatocarcinogenesis: genetic and epigenetic events. Scand. J. Gastroenterol., *34:* 737–742, 1999.

33. Yuen, M. F., Wu, P. C., Lai, V. C., Lau, J. Y., and Lai, C. L. Expression of c-Myc, c-Fos, and c-Jun in hepatocellular carcinoma. Cancer (Phila.), *91:* 106–112, 2001.

34. Takayama, T., Makuuchi, M., Hirohashi, S., Sakamoto, M., Okazaki, N., Takayasu, K., Kosuge, T., Motoo, Y., Yamazaki, S., and Hasegawa, H. Malignant transformation of adenomatous hyperplasia to hepatocellular carcinoma. Lancet, *336:* 1150–1153, 1990.

35. Sugihara, S., Nakashima, O., Kojiro, M., Majima, Y., Tanaka, M., and Tanikawa, K. The morphologic transition in hepatocellular carcinoma: a comparison of the individual histologic features disclosed by ultrasound-guided fine-needle biopsy with those of autopsy. Cancer (Phila.), *70:* 1488–1492, 1992.

36. Sun, S. Y., Kurie, J. M., Yue, P., Dawson, M. I., Shroot, B., Chandraratna, R. A. S., Hong, W. K., and Lotan, R. Differential responses of normal, premalignant, and malignant human bronchial epithelial cells to receptor-selective retinoids. Clin. Cancer Res., *5:* 431–437, 1999.

37. Li, C., and Wan, Y. J. Differentiation and antiproliferation effect of retinoic acid receptor β in hepatoma cells. Cancer Lett., *124:* 205–211, 1998.

38. Miller, W. H., Jr. The emerging role of retinoids and retinoic acid metabolism blocking agents in the treatment of cancer. Cancer (Phila.), *83:* 1471–1482, 1998.

Jpn J Clin Oncol 2003;33(6)283–287

Combined Hepatocellular and Cholangiocarcinoma: a Clinicopathologic Study of 26 Resected Cases

Yoshiko Yano[1], Junji Yamamoto[2], Tomoo Kosuge[1], Yoshihiro Sakamoto[2], Susumu Yamasaki[1], Kazuaki Shimada[1], Hidenori Ojima[3], Michiie Sakamoto[3], Tadatoshi Takayama[4] and Masatoshi Makuuchi[4]

[1]Hepatobiliary and Pancreatic Surgery Division, National Cancer Center Hospital, Tokyo, [2]Department of Surgery, Cancer Institute Hospital, Tokyo, [3]Pathology Division, National Cancer Center Research Institute, Tokyo and [4]Hepatobiliary Pancreatic Surgery Division, Graduate School of Medicine, University of Tokyo, Tokyo, Japan

Received January 10, 2003; accepted April 25, 2003

Background: Combined hepatocellular and cholangiocarcinoma (cHCC-CC) is an uncommon subtype of primary liver cancer, the clinicopathological features of which have rarely been reported in detail. The aim of this study was to clarify the characteristics of cHCC-CC in comparison with hepatocellular carcinoma (HCC) and cholangiocarcinoma (CC).
Methods: The clinicopathological features of 26 cHCC-CC patients, who were surgically treated, were reviewed by comparing them with the features of patients suffering from ordinary hepatocellular carcinoma (HCC) and cholangiocarcinoma (CC).
Results: The cHCC-CC patients showed greater similarity with HCC patients than with CC patients with regard to male/female ratio, status of hepatitis viral infection, serum alpha-fetoprotein (AFP) level, and non-tumor liver histology. The disease stage of the cHCC-CC patients was more advanced than that of either the HCC or CC patients. The cHCC-CC tumors were significantly more invasive to the portal vein than the HCC tumors and were comparable to the CC tumors. The overall 3-, 5-, and 10-year survival rates and the median survival times (95% confidence interval) were 34.6%, 23.1%, 11.5% and 1.8 (0.7–3.0) years for cHCC-CC patients, 86.7%, 66.2%, 46.8% and 4.6 (4.3–5.0) years for HCC patients, and 68.5%, 32.3%, 23.9% and 1.9 (1.1–2.7) years for CC patients, respectively. Survival of patients with cHCC-CC was significantly poorer than that of HCC or CC patients. Among the 26 patients, six survived for >5 years.
Conclusions: In most cases, cHCC-CC seems to be a variant of ordinary HCC with cholangiocellular features, rather than a true intermediate disease entity between HCC and CC. The surgical approach is recommended for selected patients with cHCC-CC.

Key words: combined hepatocellular and cholangiocarcinoma – surgery – pathology – survival – stage

INTRODUCTION

Almost all primary liver carcinomas are broadly classified either as hepatocellular carcinoma (HCC), derived from hepatocytes, or cholangiocarcinoma (CC), arising from intrahepatic bile duct epithelium. A few cases involving both hepatocellular and cholangiocellular components in the same tumor have been designated as 'combined hepatocellular and cholangiocarcinoma (cHCC-CC),' and 1.0–4.7% of such cases have been reported among primary liver cancer patients (1–7). While HCC and CC differ in their etiological, epidemiological and clinical features (8,9), the characteristics of patients with cHCC-CC have rarely been reported in detail (2,3,5–7,10). The aim of this study was to clarify the characteristics of cHCC-CC by comparing the background clinical factors, pathologic findings, and surgical outcomes of 26 resected cHCC-CC cases with those of ordinary HCC and CC cases.

For reprints and all correspondence: Junji Yamamoto, 1-37-1 Kami-Ikebukuro, Toshima-ku, Tokyo 170-8455, Japan.
E-mail: jyamamoto@jfcr.or.jp

PATIENTS AND METHODS

Patients

We reviewed 1174 cases of primary liver cancer that were surgically resected at the Department of Surgery, National Cancer Center Hospital, between January 1978 and December 1998. Of these, 1093 cases were diagnosed as HCC, 53 as CC, and 28 (2.4%) as cHCC-CC. According to Allen and Lisa (1), patients with cHCC-CC were grouped into three subtypes; type A:

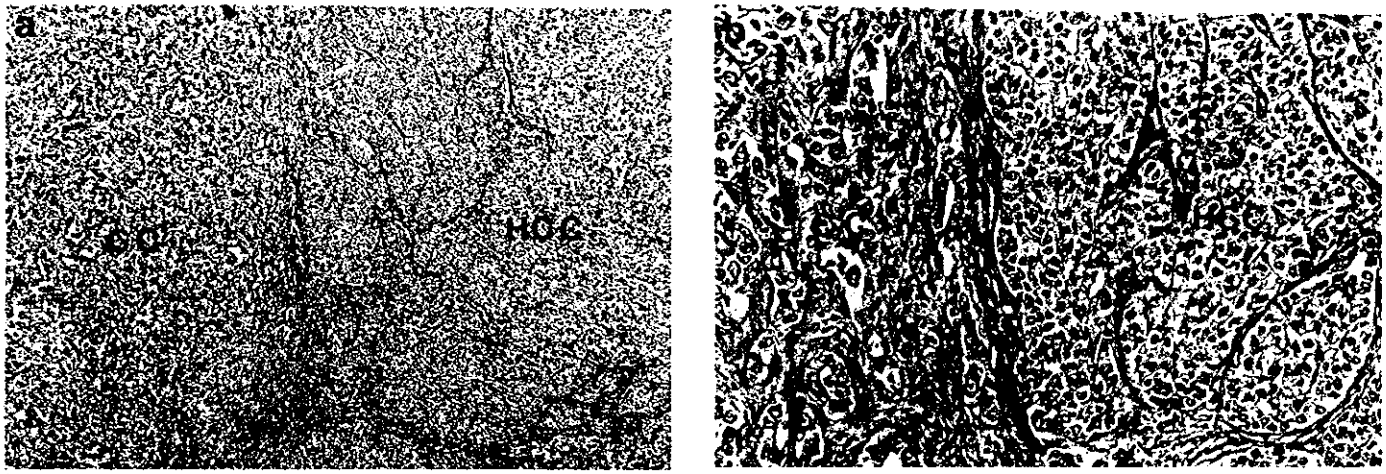

Figure 1. (a) Combined hepatocellular and cholangiocarcinoma. The tumor containing glandular structure (left) and that showing trabecular structure (right) fuses with transitional zone. (×40); (b) A part of cholangiocarcinoma shows mesotubular gland formation with desmoplastic stroma (left) and that of hepatocellular carcinoma (right) reveals thick trabecular pattern with clear cell change corresponding to Edmondson's grade III (×200).

separate masses constituting either HCC or CC (double cancer) (one patient), type B: contiguous but independent masses of HCC and CC (combined type) (one patient), and type C: an intimate intermingling of hepatocellular and glandular elements (mixed type) (26 patients). In the current study, only type C tumors were included to simply and rigorously analyze the characteristics of combined tumors. The histopathological definition of cHCC-CC was based on the criteria proposed by the World Health Organization (11): a hepatocellular element showing bile production, an intercellular bile canaliculi or trabecular growth pattern, and a cholangiocellular component showing mucin production (confirmed by periodic acid–Schiff or Alcian blue stain) or definite gland formation (Fig. 1). When a definite diagnosis was difficult, further immunoreactivity studies were conducted for carcinoembryonic antigen (CEA), carbohydrate antigen 19–9 (CA19-9), and cytokeratins (CK7 and CK19) to confirm the CC component, and for alpha-fetoprotein (AFP) to confirm the HCC component.

A diagnosis of combined HCC-CC was established when a significant amount of both HCC and CC components (>10%) was confirmed in one tumor.

Factors Analyzed

The case records of patients who underwent surgery for cHCC-CC, HCC and CC were reviewed and compared for the following variables: age, sex, serum hepatitis B surface antigen (HBsAg) and serum hepatitis C virus antibody (HCV) status, and serum AFP (normal value <20 ng/ml) and CEA levels (normal value <5 ng/ml). The pathologic findings of the resected specimens were also comparatively analyzed with regard to the number, size, and intrahepatic distribution of the tumor(s); the status of portal vein invasion, bile duct invasion, lymph node metastasis, intrahepatic metastasis, capsule formation, noncancerous liver parenchyma, and the pTNM stage. The survival rate was calculated from the date of surgery to the date of death or the last follow-up. These factors were analyzed with respect to their prognostic significance for survival.

Statistical Analysis

Cumulative overall survival rates were calculated using the Kaplan–Meier method, and differences in survival rates were assessed using the log-rank test. Differences in proportion were tested by the chi-square test. Differences in the means of each subgroup were tested using the Student's *t*-test. Significance levels were set at $P < 0.05$.

RESULTS

Patient Characteristics

Combined HCC-CC patients showed greater similarity with HCC patients than with CC patients in terms of sex ratio, hepatitis viral infection status, and frequency of elevated serum AFP values (Table 1). The surgical procedures used in the case of 26 patients with cHCC-CC included an extended hemihepatectomy for four patients (15%), a hemihepatectomy for two patients (8%), resection of a single Healey segment for six patients (23%), resection of a single Couinaud segment for six patients (23%), and a limited resection for eight patients (31%).

Pathological Features

Based on the number, size, and lobar distribution of tumors, patients with cHCC-CC had more advanced tumors than those with HCC or CC. Combined tumors were also significantly more invasive to the portal vein than HCC tumors and were comparable to CC tumors in this regard. With respect to the status of bile duct invasion, regional lymph node metastases and capsule formation, combined tumors exhibited intermediate features, between those of HCC and CC. While cHCC-CC and HCC tumors arose from cirrhotic liver conditions with the same frequency, 23% of cHCC-CC tumors originated from normal liver conditions (Table 1).

Table 1. Comparison of clinicopathologic features in cHCC-CC, HCC, and CC patients

Factors	cHCC-CC	HCC	CC	P[a]
No. of patients (%)	n = 26	n = 1093	n = 55	
Age (yrs) (median, range)	57 (27–74)	61 (16–84)	63 (40–81)	
Sex				
Male	23 (88%)	902 (83%)	35 (66%)	1–2) 0.60
Female	3 (12%)	191 (17%)	18 (34%)	2–3) 0.002
				1–3) 0.06
Viral infection[b]				
Negative	3 (12%)	152 (14%)	32 (60%)	1–2) 0.44
Hepatitis B	7 (27%)	172 (16%)	9 (17%)	2–3) <0.0001
Hepatitis C	10 (38%)	526 (48%)	5 (9%)	1–3) 0.0002
B & C	0 (0%)	16 (1%)	1 (2%)	
Unknown	8 (23%)	227 (21%)	6 (11%)	
AFP (ng/ml)				
Median (range)	75.5 (0–3 366 600)	44.1 (0–749 626)[c]	4.0 (10–369)	
<20	8 (31%)	411 (38%)	37 (86%)	1–2) 0.09
20–200	13 (50%)	323 (30%)	4 (9%)	2–3) <0.0001
≥200	5 (19%)	335 (31%)	2 (5%)	1–3) <0.0001
CEA (ng/ml) (%)				
Median (range)	3.6 (0.8–12.8)	2.9 (0–214)[d]	2.8 (4.0–479)	1–2) 0.21
<5	18 (69%)	815 (79%)	39 (74%)	2–3) 0.31
≥5	8 (31%)	211 (21%)	14 (26%)	1–3) 0.69
Noncancerous liver parenchyma				
Normal	6 (23%)	68 (6%)	47 (89%)	1–2) 0.002
Chronic hepatitis	6 (23%)	432 (40%)	5 (9%)	2–3) <0.0001
Cirrhosis	14 (54%)	593 (54%)	1 (2%)	1–3) <0.0001
Tumor number				
Solitary	8 (31%)	565 (52%)	28 (53%)	1–2) 0.04
Multiple	18 (69%)	528 (48%)	25 (47%)	2–3) 0.87
				1–3) 0.06
Tumor size (cm)				
Mean ± SE[e]	6.0 ± 4.4	4.5 ± 3.5	5.7 ± 3.0	
<3	3 (11%)	404 (37%)	2 (4%)	1–2)[f] 0.05, 0.07
3/686	14 (54%)	458 (40%)	33 (62%)	2–3)[f] <0.0001, 0.02
≥6	9 (35%)	251 (23%)	18 (34%)	1–3)[f] 0.39, 0.17
Intrahepatic distribution				
Unilobar	15 (58%)	891 (82%)	47 (89%)	1–2) 0.002
Bilobar	11 (42%)	202 (18%)	6 (11%)	2–3) 0.19
				1–3) 0.002
Portal vein invasion				
Absent	11 (42%)	650 (58%)	17 (32%)	1–2) 0.02
Present	15 (58%)	463 (42%)	36 (68%)	2–3) <0.0001
Microscopic	10 (39%)	398 (36%)	26 (49%)	1–3) 0.62
Macroscopic	5 (19%)	65 (6%)	10 (19%)	
Bile duct invasion				
Absent	19 (73%)	1011 (97%)[g]	19 (36%)	1–2) <0.0001
Present	7 (27%)	30 (3%)	34 (64%)	2–3) <0.0001
				1–3) 0.002
Lymph node metastases				
Absent	24 (92%)	1077 (99%)[h]	35 (66%)	1–2) 0.01
Present	2 (8%)	9 (1%)	18 (34%)	2–3) <0.0001
				1–3) 0.02
Capsule formation				
Absent	14 (54%)	187 (17%)	49 (92%)	1–2) <0.0001
Present	12 (46%)	906 (83%)	4 (8%)	2–3) <0.0001
				1–3) 0.0002
pTNM				
I	0	96	0	1–2) <0.0001
II	3	318	9	2–3) <0.0001
IIIA	6	444	16	1–3) <0.0001
IIIB	1	6	12	
IVA	16	229	16	
IVB	0	0	0	

[a]Differences in proportion were tested using a chi-square test. Differences in the means of each subgroup were tested using the Student's *t*-test. Significance levels were set at $P < 0.05$. 1–2), 2–3), and 1–3) refers to a comparison between the cHCC-CC group and the HCC group, the HCC group and the CC group and the cHCC-CC group and the CC group, respectively. [b]Chi-square test, excluding unknown cases. [c]Data not available for 24 patients. [d]Data not available for 67 patients. [e]Standard error. [f]Tested by chi-square test and Student's *t*-test. [g]Data not available for 52 patients. [h]Data not available for seven patients.

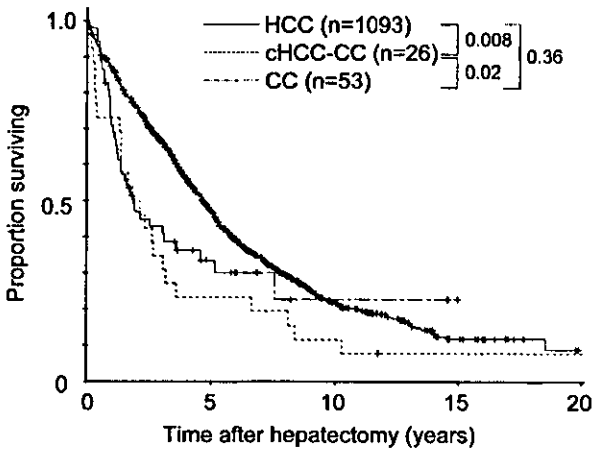

Figure 2. Comparison of cumulative survival rates among patients with cHCC-CC, HCC, and CC. Patients with cHCC-CC had a significantly poorer survival than HCC and CC patients.

Detailed Profiles of Patients with Multiple Tumors

Among the 18 patients with multiple tumors, eight had two tumors, two had three tumors, and the other eight had four or more deposits. All ten patients with three or more deposits and two patients with two nodules had multiple tumors on an intrahepatic metastasis basis. The background liver tissue was normal in three patients, while four patients had chronic hepatitis and three patients had cirrhosis. Five of the remaining six patients with two deposits had a distinct HCC nodule in a cirrhotic liver, while the sixth patient had them in chronic hepatitis. The maximum tumor size of cHCC-CC ranged from 2.1 to 17 cm.

Overall Survival After Hepatectomy and Pattern of Recurrence

Three in-hospital deaths occurred (in-hospital mortality rate = 11.5%); two patients died from hepatic failure 25 and 92 days after surgery. Another patient died from aggressive tumor recurrence 118 days after hepatectomy. The overall 3-, 5-, and 10-year survival rates and the median survival times (95% confidence interval) were 34.6%, 23.1%, 11.5% and 1.9 (0.70–3.0) years for cHCC-CC patients, 86.7%, 66.2%, 46.8% and 4.6 (4.3–5.0) years for HCC patients, and 68.5%, 32.3%, 23.9% and 1.86 (1.1–2.7) years for CC patients, respectively. Survival of patients with cHCC-CC was significantly poorer than that of HCC or CC patients. Among the 26 patients, six survived for >5 years, and five eventually died from tumor recurrence (Fig. 2). By univariate analysis, the macroscopic vascular invasion ($P = 0.004$) and bilobar tumor ($P = 0.05$) were found to be significant predictors of poor outcome. Tumor size (<6 cm vs. ≥6 cm) was a marginally significant factor for survival ($P = 0.06$). Other factors including number of tumors, and surgical margin were not associated with reduced survival after surgery. Recurrence was not evaluated in the case of two patients who died in the hospital and in the case of three patients who died during the follow-up period. Among the remaining 21 patients, 20 (95%) developed recurrence. The sites of recurrence were the remnant liver (15), lymph node (2), lung (3), bone (1) and right adrenal gland (1). Metastatic lymph node tumors were made up of cHCC-CC cells in one patient and CC cells in another. The adrenal gland metastasis was made up of cHCC-CC cells. In cases of recurrence, the median time (range) for the event was 10 months (0.4–173 months).

DISCUSSION

The ratio of ordinary HCC to cHCC-CC tumors reportedly varies between 17:1 in an autopsy series (2) and 35:1 in a clinical series (3). In an earlier study, the ratio in surgically resected series was 27:1 (5), while the ratio in the present series was 39:1. The true incidence is likely to be much higher than that of the surgical series because in both, our series and the earlier report, patients with cHCC-CC were at a more advanced stage of the disease than those with ordinary HCC (5).

Goodman et al. (3) identified criteria, different from Allen and Lisa's definition, for a pathomorphological diagnosis of cHCC-CC, and classified this disease into three subtypes, based on histological patterns. According to this classification, type I, 'collision tumors,' contain separate and apparently coincidental areas of HCC and CC, including tumors in different parts of the liver; type II, 'transitional tumors,' exhibit hepatocellular differentiation, with transition areas to adenocarcinoma or to a mixed hepatocellular glandular tumor; and type III, 'fibrolamellar tumors,' exhibit a combination of hepatocellular and cholangiocellular differentiation throughout the tumor, without separate areas of one or the other. Goodman's type I tumor corresponds to Allen and Lisa's type A and type B. Type III tumor, however, is not equivalent to Allen and Lisa's type C but represents a special variant of fibrolamellar HCC. In the current study, combined tumors, classified as Allen and Lisa's type C or Goodman's type II, were included to make a simple and strict interpretation of the results.

With regard to the histogenesis of Allen and Lisa's type C or Goodman's type II combined tumor, the following possibilities have been proposed (12): (1) the CC component arises from the main HCC tumor, and (2) the entire cancer arises from a stem cell potentially differentiating into hepatocytes and bile duct epithelium. Based on the similarity in the clinicopathological characteristics (average age, male/female ratio, hepatitis viral positivity, serum AFP level, and the presence of cirrhosis) of the two diseases, some researchers (2,5,12) have speculated that the CC components in the cHCC-CC tumors were those transformed from part of the HCC tumors. In the present series, a similarity in the clinical backgrounds of the cHCC-CC patients seems to indicate that cHCC-CC represents a variant of ordinary HCC that exhibits cholangiocellular metaplasia, rather than a true intermediate disease entity between HCC and CC, as previously reported in several studies (3,5). Imai et al. (13) showed the same p53 gene mutational pattern in both HCC and CC components, and the same Rb-1 locus replication error pattern in both components in some patients with cHCC-CC, thus providing genetic evidence that both components had

the same origin. However, the reports mentioned above are from Asia, where the instances of HCCs, caused by a virus-infected liver, are greater than in western countries. Recently, Jarnagin et al. (7) reported a large western series of cHCC-CC, which were selected on the basis of a rigorous pathological definition. It is noteworthy that the clinical background of patients with combined tumors was most similar to that of CC patients. The lack of an association between chronic liver disease and cHCC-CC in the western series indicated the presence of other histogenesis mechanisms. In our study, cHCC-CC was detected more frequently in normal liver conditions than in a HCC condition, although the frequency of viral infection was similar. Yano et al. (14) established a human cHCC-CC cell line expressing the functional characteristics of HCC on a plastic dish, which was capable of producing adenocarcinoma features in the subcutaneous tissue of nude mice. Kobrechts et al. (15) have reported a primary liver tumor made up of immature cells displaying features of both hepatocytes and bile duct epithelial cells, thereby suggesting the presence of stem cells in the human liver. These data suggest the possible existence of an amphi-potential progenitor cell.

Vascular invasion by HCC always appears in the form of an intravascular tumor thrombus, which is one of the most conspicuous growth patterns of this disease (16). In contrast, CC invades the connective tissue of the portal triad, obstructing or narrowing the lumen of the invaded vessels (17). In the present series, among the 15 cHCC-CC patients with portal vein invasion, five exhibited a macroscopic portal vein thrombus, showing the same mode of portal vein invasion as HCC tumors. Regional lymph node metastases were observed in two patients at the time of the initial hepatectomy and in two patients as a post-resection recurrence; thus, cHCC-CC tumors have a higher propensity towards the lymphatic system than HCC tumors. The intermediate frequency of bile duct invasion and capsule formation also indicated that established cHCC-CC tumors seemed to exhibit the invasive characteristics of both HCC and CC tumors.

Combined HCC-CC patients showed a significantly poorer rate of survival after surgery than patients with either HCC or CC. A western series indicated a much better post-resection outcome for larger combined tumors (8). And in their report, there was no difference in survival rates among cHCC-CC, HCC and CC patients. The difference in the results in the current series might be explained by the fact that the tumor stage observed in patients with cHCC-CC was more advanced than that in HCC and CC patients. In addition, the degree of compromised liver function was greater in cHCC-CC patients than in CC patients. In addition, in cases of HCC arising in the cirrhotic liver, the patient's life is continuously jeopardized by recurrence as a result of multifocal tumor occurrence from the carcinogenic background liver, even if the initial tumor nodule is completely removed by surgical resection (18,19). The linear declines in the 5-year survival curves in patients with HCC or cHCC-CC were clearly different from that in CC patients. This may be due to a similarity in virus status and the presence of cirrhosis in these two groups.

No report has been published about nonsurgical therapy for cHCC-CC. Considering that six patients survived for >5 years (two of whom survived for >10 years) after surgery, a surgical approach, if possible, is presently the best treatment available for cHCC-CC.

Acknowledgment

This study was supported by a Grant-in-Aid for Cancer Research from the Ministry of Health, Labor and Welfare, Japan.

References

1. Allen RA, Lisa JR. Combined liver cell and bile duct carcinoma. *Am J Pathol* 1949;25:647–55.
2. Edmondson H, Peters RL. Neoplasms of the liver. Disease of the liver, 5th Ed. In: L. Schiff and E. Schiff, editors. Philadelphia, PA: Lippincott 1982.
3. Goodman Z, Ishak KG, Langloss JM, Sesterhenn IA, Kabin L. Combined hepatocellular-cholangiocarcinoma. A histologic and immunohistochemical study. *Cancer* 1985;55:124–35.
4. The Liver Cancer Study Group of Japan. Primary liver cancer in Japan. *Ann Surg* 1990;211:277–87.
5. Maeda T, Adachi E, Kajiyama K, Sugimachi K, Tsuneyoshi M. Combined hepatocellular and cholangiocarcinoma: proposed criteria according to cytokeratin expression and analysis of clinicopathologic features. *Human Pathol* 1995;26:956–64.
6. Ng IO, Shek T W, Nicholls J, Ma L1. Combined Hepatocellular-cholangiocarcinoma: a clinicopathological study. *J Gastroenterol Hepatol* 1998;13: 34–40.
7. Jarnagin WR, Weber S, Tickoo SK, Koea JB, Obiekwe S, Fong Y, et al. Combined hepatocellular and cholangiocarcinoma: demographic, clinical, and prognostic factors. *Cancer* 2002;94:2040–6.
8. Edmondson HA, Steiner P. Primary carcinoma of the liver: a study of 100 cases among 48,900 necropsies. *Cancer* 1954;7:462–503.
9. Anthony PP. Hepatic neoplasms. In: MacSween RNM, Anthony PP, Scheuer PJ, editors. Pathology of the Liver. Edinburgh: Churchill Livingstone 1979;587–613.
10. Aoki K, Takayasu K, Kawano T, Muramatsu Y, Moriyama N, Wakao F, et al. Combined hepatocellular carcinoma and cholangiocarcinoma: clinical features and computed tomographic findings. *Hepatology* 1995;18:1090–5.
11. Gibson J. Histological typing of tumors of the liver, biliary tract, and pancreas. Geneva, Switzerland: World Health Organization 1978.
12. Kojiro M. Pathomorphology of advanced hepatocellular carcinoma. Primary liver cancer in Japan. In: T. Tobe, et al. editors. Tokyo: Springer-Verlag 1992;31–7.
13. Imai Y, Oda H, Arai M, Shimizu S, Nakatsuru Y, Inoue T, et al. Mutational analysis of the p53 and K-ras genes and allelotype study of the Rb-1 gene for investigating the pathogenesis of combined hepatocellular-cholangiocellular carcinomas. *JJCR* 1996;87:1056–62.
14. Yano H, Iemura A, Haramaki M, Momosaki S, Ogasawara S, Higaki K, et al. A human combined hepatocellular and cholangiocarcinoma cell line (KMCH-2) that shows the features of hepatocellular carcinoma or cholangiocarcinoma under different growth conditions. *J Hepatol* 1996;24:413–22.
15. Kobrechts C, De Vos R, Van den Heuvel M, Van Cutsem E, Van Damme B, Desmet V, et al. Primary liver tumor of intermediate (hepatocyte-bile duct cell) phenotype: a progenitor cell tumor? *Liver* 1998;18:288–95.
16. Albacete RA, Matthews MJ, Saini N. Portal vein thromboses in malignant hepatoma. *Ann Intern Med* 1967;67:337–48.
17. Weinbren K, Mutum SS. Pathological aspects of cholangiocarcinoma. *J Pathol* 1983;139:217–29.
18. Kosuge T, Makuuchi M, Takayama T, Yamamoto J, Shimada K, Yamazaki S. Long-term results after resection of hepatocellular carcinoma: experience of 480 cases. *Hepato-gastroenterol* 1993;40:328–32.
19. Yamamoto J, Kosuge T, Takayama T, Shimada K, Yamasaki S, Ozaki H, et al. Recurrence of hepatocellular carcinoma after surgery. *Br J Surg* 1996;83:1219–22.

[CANCER RESEARCH 64, 7263–7270, October 15, 2004]

Distinct Chromosomal Bias of Gene Expression Signatures in the Progression of Hepatocellular Carcinoma

Yutaka Midorikawa,[1,3] Shuichi Tsutsumi,[1] Kunihiro Nishimura,[2] Naoko Kamimura,[1] Makoto Kano,[2] Hirohiko Sakamoto,[4] Masatoshi Makuuchi,[3] and Hiroyuki Aburatani[1]

[1]Genome Science Division, [2]Intelligent Cooperative Systems Division, Research Center for Advanced Science and Technology, and [3]Hepato-Biliary-Pancreatic Surgery Division, The University of Tokyo, Tokyo; and [4]Department of Surgery, Saitama Cancer Center, Saitama, Japan

ABSTRACT

To identify the chromosomal aberrations associated with the progression of liver cancer, we applied expression imbalance map analysis to gene expression data from 31 hepatocellular carcinomas and 19 noncancerous tissues. Expression imbalance map analysis, which detects mRNA expression imbalance correlated with chromosomal regions, showed that expression gains of 1q21-23 (74%), 8q13-21 (48%), 12q23-24 (41%), 17q12-21(48%), 17q25 (25%), and 20q11 (22%) and losses of 4q13 (48%), 8p12-21 (32%), 13q14 (32%), and 17p13 (29%) were significantly associated with hepatocellular carcinoma. Most regions with altered expression identified by expression imbalance map were also identified in previous reports using comparative genomic hybridization. We demonstrated chromosomal copy number gain in 1q21-23 and loss in 17p13 by genomic quantitative PCR, suggesting that gene expression profiles reflect chromosomal alterations. Furthermore, expression imbalance map analysis revealed that more poorly differentiated hepatocellular carcinoma contain more chromosomal alterations, which are accumulated in a stepwise manner in the course of hepatocellular carcinoma progression: expression imbalance of 1q, 8p, 8q, and 17p occur as early events in hepatocarcinogenesis, and 12q, 17q25 and 20q occur as later events. In particular, expression gain of 17q12-21 and loss of 4q were seen to accumulate constantly through the dedifferentiation process. Our data suggest that gene expression profiles are subject to chromosomal bias and that expression imbalance map can correlate gene expression to gene loci with high resolution and sensitivity.

INTRODUCTION

Hepatocellular carcinoma develops with dedifferentiation after liver injury by chronic hepatitis viral infection. In multistep hepatocarcinogenesis, several molecular events accumulate in a fashion that parallels the clinical progression of liver cancer (1, 2). Some studies have tried to identify the genes altered in dedifferentiation of hepatocellular carcinoma using samples with a nodule-in-nodule appearance (2, 3). Still, little is known about the genes that play a pivotal role during the course of liver cancer progression.

Genomic amplification of oncogenes and inactivation of tumor suppressor genes are frequently associated with cancer progression. Comparative genomic hybridization (CGH) has contributed to our basic cancer understanding and diagnosis of cancer (4) but can only detect genomic alterations > 20 Mb. This low resolution makes it difficult for CGH to identify genes differentially expressed in carcinogenesis. To detect amplification events involving small genomic regions, high-resolution analysis of DNA copy number variation using cDNA microarrays has been used (5–7). However, because this technology only analyzes genomic DNA, supplementary experiments are required to confirm the expression of candidate genes in tumorigenesis. Microarrays have also been used to obtain comprehensive measurements of genome-wide expression profiles. Using such techniques, classification of cancer specimens or identification of gene sets for carcinogenesis and cancer progression have been reported by many researchers (2, 8–11).

Information about genome dosage and transcriptome may be obtained through microarray technologies if gene expression and gene localization data are integrated. In our study of oligodendroglioma, we showed that biological differences between genetic subsets of oligodendroglioma are reflected in their gene expression profiles and that genomic copy number alteration consistently accompanies perturbation of the transcriptome (12). Similarly, Virtaneva *et al.* (13) demonstrated an association between trisomy 8 and overexpression of genes on chromosome 8 in acute myeloid leukemia, and Tay *et al.* (11) performed CGH and expression microarray using gastric cancer specimens integrating CGH data with the microarray results.

Recently, based on mRNA expression, we have reported a method for constructing a transcriptome map (14). The expression imbalance map is a visualization method for detecting expression imbalance in regions of chromosomes. It extends beyond simple spatial mapping of microarray expression profiles on chromosomal locations to profile genomic losses and gains at a much higher resolution than CGH. In the expression imbalance map, signal noise can be reduced using a moving average compared with conventional methods, and users can determine thresholds. Furthermore, the expression imbalance map not only detects the expression imbalance frequency across all cases but also detects individual differences between cancer specimens. In addition, the expression imbalance map allows observation of both expression imbalance and the expression of each gene simultaneously. We previously applied the expression imbalance map to gene expression data derived from squamous cell lung carcinoma and detected, as regional signal images, several novel and many known loci with frequent genomic losses or gains on various chromosomes (14).

In the present study, we have focused on chromosomal bias in transcripts during multistep hepatocarcinogenesis. We applied the expression imbalance map method to gene expression data of hepatocellular carcinoma and observed a stepwise change of expression along at defined chromosomal loci in liver cancer progression. Genomic quantitative PCR (qPCR) analysis confirmed that expression imbalance map data correlated with genomic aberrations. The novel regions identified by the expression imbalance map may play pivotal roles during the course of dedifferentiation of hepatocellular carcinoma and likely contain some candidate genes responsible for liver cancer progression.

MATERIALS AND METHODS

Patients and Tissue Samples. Thirty-one patients with hepatocellular carcinoma undergoing hepatectomy in the Hepato-Biliary-Pancreatic Surgery Division, Department of Surgery, Graduate School of Medicine, University of

Received 4/17/04; revised 8/3/04; accepted 8/10/04.

Grant support: Grant-in-Aid for Scientific Research (B) 12557051 and 13470114 and Scientific Research on Priority Areas (C) 12217031 from The Ministry of Education, Science, Sports and Culture (H. Aburatani), Health and Labor Sciences Research Grants on Hepatitis and BSE and The Mitsubishi Foundation (H. Aburatani), and Mitsui Life Social Welfare Foundation (Y. Midorikawa).

The costs of publication of this article were defrayed in part by the payment of page charges. This article must therefore be hereby marked *advertisement* in accordance with 18 U.S.C. Section 1734 solely to indicate this fact.

Requests for reprints: Hiroyuki Aburatani, Genome Science Division, Research Center for Advanced Science and Technology, The University of Tokyo, 4-6-1 Komaba, Meguro-ku, Tokyo 153-8904, Japan. Phone: 81-3-5452-5352; Fax: 81-3-5452-5355; E-mail: haburata-tky@umin.ac.jp.

Tokyo, or the Department of Surgery, Saitama Cancer Center, were included in this study with informed consent. Among the 31 patients with hepatocellular carcinoma, 10 were positive for hepatitis B surface antigen and 21 for hepatitis C viral antibody. GeneChip analysis was performed using 50 samples, including 31 hepatocellular carcinomas and 19 surrounding noncancerous tissues. Clinical factors and tumor status based on histologic findings of resected specimens are summarized in Table 1.

The surgical specimens were immediately cut into small pieces after resection, snap frozen in liquid nitrogen and stored at −80°C.

RNA Extraction and Oligonucleotide Microarray. Total RNA was isolated from frozen tissue using Isogene (Nippon Gene, Tokyo, Japan), according to the manufacturer's protocol. Experimental procedures for GeneChip were performed according to GeneChip Expression Analysis Technical Manual (Affymetrix, Santa Clara, CA), using 15 μg of total RNA. Samples were analyzed on U95A array chips (Affymetrix).

Normalization and Filtering of Intensity of Gene Expression. Before analysis, we normalized and filtered the raw data. A quantile normalization procedure was used for the probe intensity distribution across different chips. The average of expression level intensity, the average difference, was scaled to 100, and for each expression data set, where the average difference values lay outside the range (1 to 10,000), the values was reset to a minimum 1 and to a maximum of 10,000. Genes where the coefficient of variation through all of the samples was <0.3 were excluded from analysis. Subsequently, all values were log-transformed for additional analysis.

Expression Imbalance Map. The expression imbalance map was applied to gene expression data of hepatocellular carcinoma and noncancerous tissues obtained by microarray. Gene locus information was obtained from the web sites for Genes On Sequence Map (*Homo sapiens* build 33). The basic concept and method of expression imbalance map are described elsewhere (14). Briefly, gene expression levels of cancer specimens were compared with the average of noncancerous tissues, and the regions in which the numbers of up-regulated or down-regulated genes were significantly concentrated were mapped on the chromosomal region and constitute an expression imbalance map.

Table 1 *Clinical factors and tumor status based on histologic findings of resected specimens*

Sample no.	Age (y)	Gender	Hepatitis virus	Differentiated grade	Tumor size (mm)	fc	sf	vv	vp	b	im	s
w1	48	M	HB	WD	22	−	+	−	−	−	−	−
w2	72	F	HC	WD	33	−	+	−	−	−	−	−
w3	62	M	HB	WD	31	−	+	−	−	−	−	−
w4	66	F	HC	WD	40	−	+	−	−	−	−	−
w5	65	M	HC	WD	27	+	+	−	−	−	−	−
w6	75	M	HC	WD	40	+	+	−	−	−	−	−
w7	68	F	HB	WD	10	−	−	−	−	−	−	−
w8	60	M	HC	WD	14	−	−	−	−	−	−	−
w9	66	M	HC	WD	36	+	−	−	+	+	+	−
w10	66	M	HC	WD	48	+	−	−	−	−	+	−
m1	69	F	HB	MD	38	+	−	−	−	−	−	−
m2	71	M	HC	MD	15	−	+	−	−	−	−	−
m3	47	M	HB	MD	24	+	+	−	+	+	−	−
m4	71	F	HC	MD	22	−	+	−	−	−	−	−
m5	71	F	HC	MD	30	+	+	−	−	−	−	+
m6	69	M	HC	MD	50	+	+	−	−	−	−	−
m7	70	F	HC	MD	23	−	+	−	−	−	−	−
m8	53	M	HB	MD	45	+	+	−	−	−	−	−
m9	63	F	HC	MD	20	+	+	−	−	−	−	−
m10	50	M	HB	MD	25	−	+	−	+	−	−	−
m11	70	M	HC	MD	20	+	−	−	−	−	−	−
m12	49	M	HB	MD	22	−	+	−	+	−	+	−
m13	62	M	HC	MD	50	+	+	−	−	−	−	−
p1	54	M	HB	PD	11	−	+	−	−	−	−	−
p2	65	M	HC	PD	35	+	−	−	−	−	+	+
p3	56	F	HB	PD	45	−	−	−	−	−	−	+
p4	70	F	HC	PD	30	−	−	+	−	−	−	−
p5	63	M	HC	PD	40	+	+	−	−	−	−	−
p6	72	M	HC	PD	110	−	−	−	−	−	−	+
p7	70	M	HC	PD	45	+	−	−	−	−	−	−
p8	60	M	HC	PD	85	+	+	−	+	+	+	−

Abbreviations: fc, capsule formation; sf, septum formation; vv, tumor thrombus in hepatic vein; vp, tumor thrombus in portal vein; b, tumor thrombus in bile duct; im, intrahepatic metastasis; s, serosal invasion; M, male; F, female; HB, hepatitis B virus infection; HC, hepatitis C virus infection; WD, well differentiated HCC; MD, moderately differentiated HCC, PD; poorly differentiated HCC.

On the basis of the statistical probability, P, of rank sum, the differential level E value was defined as follows: $E = -\log_{10}P$.

The chromosomal regions with expression gain or loss were defined according to both E value and range of alteration of gene expression.

Clustering Hepatocellular Carcinoma Samples Using Chromosomal Regions with Expression Imbalance. A heat map was constructed using expression imbalance map-positive chromosomal regions as binary variables. Hepatocellular carcinoma samples were arranged in order of the total number of positive regions, and the samples with less than two positive regions were defined as group1, three or four positive regions as group 2, and more than five positive regions as group3. Next, considering the length of positive regions, expression imbalance in each 100-kb region was calculated, and the sum of the length of positive chromosomal change in each sample was displayed graphically as the intensity of red or blue. Thirty-one tumor samples were arranged in accordance to tumor differentiation grade, and the total length of transcriptome alterations in each sample were compared by ANOVA.

DNA Extraction and qPCR. Genomic DNA was extracted from fresh-frozen tissue, using the QIAamp DNA Mini kit (Qiagen, Valencia, CA), according to the manufacturer's instructions. PCR amplification was performed using Taq Polymerase and 20 ng of sample DNA. Oligonucleotide primers were designed to amplify genomic DNA fragments near the chromosomal locus of 1q21-23, encoding *CCT3* (145 bp), *PSMB4* (115 bp), 12q23-24, encoding *CKAP4* (141 bp), *UNG* (140 bp), 17p13, encoding *ASGR1* (136 bp), *DKFZP566H073* (168 bp), and β-actin (132 bp) as a control reference. The primers used were as follows: *CCT3*, 5′-TGACATCGTTTCAGGCCAC-3′ and 5′-GCACTCTGGCTCAGGAAAAG-3′; *PSMB4*, 5′-TGGCTCGTTTCCGCAACATC-3′ and 5′-ACCATCTGGCCGAGAACTTG-3′; *CKAP4*, 5′-GTGCAGTCTTTGCAAGCCAC-3′ and 5′-CTGGAGTTTCTGCAGCACTTC-3′; *UNG*, 5′-TGCTTAGAAAGGTCCCCTTG-3′ and 5′-GGCCAGATTCTGGAAAGTTG-3′; *ASGR1*, 5′-TCCACGTGAATCTGCACCTC-3′ and 5′-GAGCTCAGCTGCTGGATATC-3′; *DKFZP566H073*, 5′-AGACCTGCCCCATTTGCAAG-3′ and 5′-CAAAGGAGGTGGGAAGAGTG-3′; and β-actin, 5′-GACCTGACTGACTACCTCATG-3′ and 5′-CATCTCTTGCTCGAAGTCCAG-3′. qPCR for detecting gain of chromosome 1q21-23 and 12q23-24 and loss of chromosome 17p13 were performed using an iCycler (Bio-Rad, Hercules, CA). The relative quantification is given by the ratio between the mean value of the target gene and the mean value of β-actin in each sample.

RESULTS

Expression Imbalance Map for Detecting Expression Imbalance Regions. The expression imbalance map was applied to 31 hepatocellular carcinomas, comparing their expression data to the average of expression across 19 noncancerous tissues (Fig. 1*A*). Various criteria may be used to define expression imbalance regions. When expression imbalance regions were defined as those with E values > 2 and a region of >3.0Mb, compared with the background liver, expression gains on chromosome arms of hepatocellular carcinoma were observed on 1q21-23 (74%), 8q13-21 (48%), 12q23-24 (41%), 17q12-21 (48%), 17q25 (25%), and 20q11 (22%) and expression losses were detected on 4q13 (48%), 8p12-21(32%), 13q14 (32%), and 17p13 (29%; Fig. 1, *B* and *C*). To provide a comparison between our data and previously reported observations of chromosomal alterations of hepatocellular carcinoma obtained by CGH, chromosomal arms with expression gain or loss are summarized in Table 2. Most regions with altered expression, as determined by the expression imbalance map, were also indicated in previous reports using CGH. Notable exceptions are a gain of 12q, which has never been reported previously, and a loss of 16q, which has been demonstrated in many previous reports, but was not identified in our analysis.

Gene list of the imbalanced region is shown with their median and average signal intensities and SDs in the tumors and controls (Supplemental Fig. 1).[5]

Comparison with existing CGH data sets for hepatocellular carci-

[5] Internet address: http://www2.genome.rcast.u-tokyo.ac.jp/hcc.

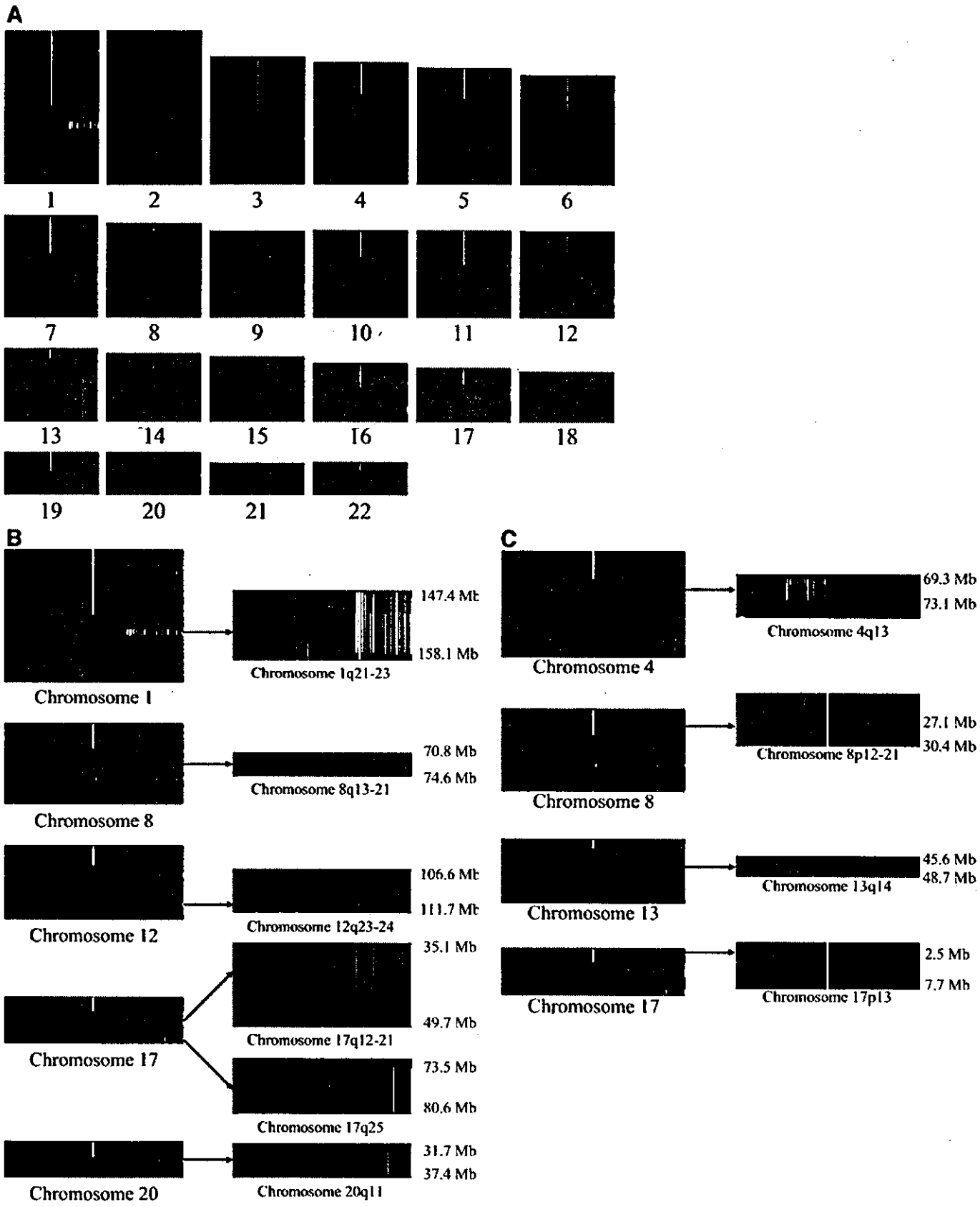

Fig. 1. Expression imbalance map for detecting expression imbalance regions in hepatocellular carcinoma. *A*. Regions of under- and overexpression in hepatocellular carcinoma were visualized on the *left side* and the *right side*, respectively, as gray regional signals. Each column represents tissue samples. The lighter areas correspond to higher probability of an expression imbalance region. The expression imbalance map enables the user to identify many more genes by referring to the more expanded area with lower luminance. This figure shows the expression imbalance at an E value > 2. *B*, expression imbalance region at an E value > 2 and a range of expression gain > 3.0 Mb. The length assigned to each chromosome is proportional to the number of Locus IDs on the chromosome. *C*, expression imbalance region at E value > 2 and a range of expression loss > 3.0 Mb.

Table 2 *Expression imbalance region and chromosomal alteration in hepatocellular carcinoma*

EIM		Others by CGH								
Chromosome		(16)	(18)	(19)	(20)	(23)	(25)	(26)	(27)	(28)
Gains										
1q	74	86	57	77	73	66	72	46	58	78
5p					38					
6p								20	33	
7q					40					
8q	48	77	52	52	83	48	48	31	60	66
11q				26						
12q	41									
17q	48		29				30	43	33	
20q	22		29			20	37			
xq					50					
Losses										
1p						36		37		
4q	48	59	33	35	40	40	43	48	70	32
5q								35		
6q			19					23	37	
8p	35	77		26	44	32	37	28	65	29
10q										17
13q	32		19	55			37	20	37	37
16p					46					
16q		50	14	52	63	70	30	33	54	46
17p	29			52	60	52		37	51	51
19p						42				
22q						28				

Expression gain or loss region by EIM was defined as E value > 2 and the range > 3.0 Mb. Figure means percentage of positive region. The number in parenthesis corresponds with reference number.

Abbreviation: EIM, expression imbalance map.

noma suggests that gene expression profiles reflect chromosomal alterations and that the expression imbalance map is a useful tool for estimating chromosomal change from expression data.

Classification of Hepatocellular Carcinomas by Chromosomal Bias of Gene Expression. Expression imbalance map analysis showed that genes with expression change are derived from particular chromosomal regions with altered copy number. To identify possible association between these chromosomal alterations and liver cancer progression, we investigated the relationship between expression imbalance and tumor differentiation grade (Fig. 2).

First, we counted the expression-positive regions by expression imbalance map and arranged the samples according to the sum of positive regions. This resulted in the identification of 9 samples that constitute the first group and contain less than two positive regions, 10 samples in the second group with three or four positive regions, and 12 samples in the third group with more than five positive regions. Interestingly, all of the samples from the first group were well differentiated, and all of the poorly differentiated samples were concentrated in the third group (Fig. 2*A*), demonstrating a distinct trend for poorly differentiated grade tumors to contain more chromosomal aberrations.

Summating the number of 100-kb regions with expression imbalance, tumor differentiation grade and total length of chromosomal change were significantly correlated: the mean length of expression changes were 9.7 ± 5.6, 28.3 ± 13.0, and 45.2 ± 7.9 Mb in well differentiated, moderately differentiated, and poorly differentiated, respectively ($P < 0.00001$ by ANOVA; Fig. 2*B*). Some chromosomal regions showed consistent relationships with tumor progression. For example, expression gains of chromosome arms were observed on 12q23-24 and 20q11 with dedifferentiation from well differentiated to moderately differentiated, whereas an expression gain of 17q25 was significantly associated with dedifferentiation from well differentiated and moderately differentiated to poorly differentiated ($P < 0.05$ by Student-Newman-Keuls test). Notably, a gain of 17q12-21 and loss of 4q13 were found in each step of tumor dedifferentiation (Fig. 2*C*).

These results suggest that expression alterations of 1q21-23, 8p12-21, 8q13-21, and 17p13 occur as early events in hepatocarcinogenesis and 4q13, 12q23-24, 17q12-21, 17q25, and 20q11 as later events. Thus, liver cancer progresses with stepwise chromosomal expression change.

Expression Imbalance Map Was Correlated with Genomic Aberrations on 1q21-23 and 17p13 by Genomic qPCR. Many genomic aberrant regions in hepatocellular carcinoma detected by the expression imbalance map in this study are the same as those identified by CGH in previous studies (Table 2). To investigate the relationship between genomic and transcriptional aberrations, genome dosage in 1q21-23, 12q23-24, and 17p13 regions was confirmed using genomic qPCR for 27 hepatocellular carcinoma and the corresponding noncancerous liver samples (15).

qPCR was performed using 27 noncancerous liver samples. Average copy numbers for the loci of *CCT3* and *PSMB4* genes were 1.28 ± 0.37 and 0.90 ± 0.22, respectively. The genome dosage of hepatocellular carcinoma tended to increase in accordance with tumor differentiation grade (Fig. 3, *A* and *B*). In particular, consistent with the expression imbalance map data ($P < 0.001$, Mann-Whitney *U* test), genome dosage, shown as relative quantification, was significantly increased in moderately differentiated and poorly differentiated compared with well differentiated, both in *CCT3* and *PSMB4*. To clarify the relationship between genome dosage and the probability of expression imbalance in the 1q21-23 region, the relative quantification between samples with E values < 3 was compared with those samples with E values > 3. As shown in the top right section of Fig. 3, the relative quantification of *CCT3* and *PSMB4* increased significantly in the higher E value group ($P < 0.05$, Mann-Whitney *U* test; Fig. 3, *A* and *B*).

Genomic loss was also detectable in 17p13 region. Consistent with the expression imbalance map data, relative quantification was significantly decreased in samples with E values > 2, compared with those with E values < 2, both in *ASGR1* and *DKFZP566H073* (Fig. 3, *C* and *D*), whereas genomic amplification on 12q23-24 was not observed by qPCR (data not shown).

Through these results, we demonstrated that genes identified by expression imbalance map had altered genome dosage with statistical significance, and alterations of their mRNA expression levels may reflect a gain or loss of genomic copy number at the locus from 147.4 to 158.1 Mb on 1q21-23 and from 2.5 to 7.7 Mb on 17p13. On the other hand, genome dosage of chromosome 12q23-24, which has never detected in the previous CGH, has no change between hepatocellular carcinoma and chronic liver disease in DNA using qPCR.

Search for Candidate Genes Responsible for Hepatocarcinogenesis and Liver Cancer Progression. To identify candidate genes responsible for hepatocarcinogenesis and liver cancer progression, we further investigated the transcription of each of 55 genes in the 1q21-23 region (147.4–158.1Mb; Fig. 4). We found four related genes that were highly expressed in hepatocellular carcinoma compared with noncancerous tissues, *HAX1* (1q22), *SHC1* (1q21), *CKS1B* (1q21), and *CCT3* (1q23). Similarly, two growth-related genes were identified on the other nine regions selected by expression imbalance map: *AATF* (17q11-12) and *TK1* (17q23-25) had increased expression compared with noncancerous tissues.

DISCUSSION

Using CGH, many investigators have already reported various chromosomal regions of hepatocellular carcinoma that undergo cytogenetic change (16–28). Consistent with the previous data, the expression imbalance map identified an increase in gene expression on chromosomes 1q, 8q, 17q, and 20q and a decrease on 4q, 8p, 13q, and 17p. To validate the relationship between expression imbalance and

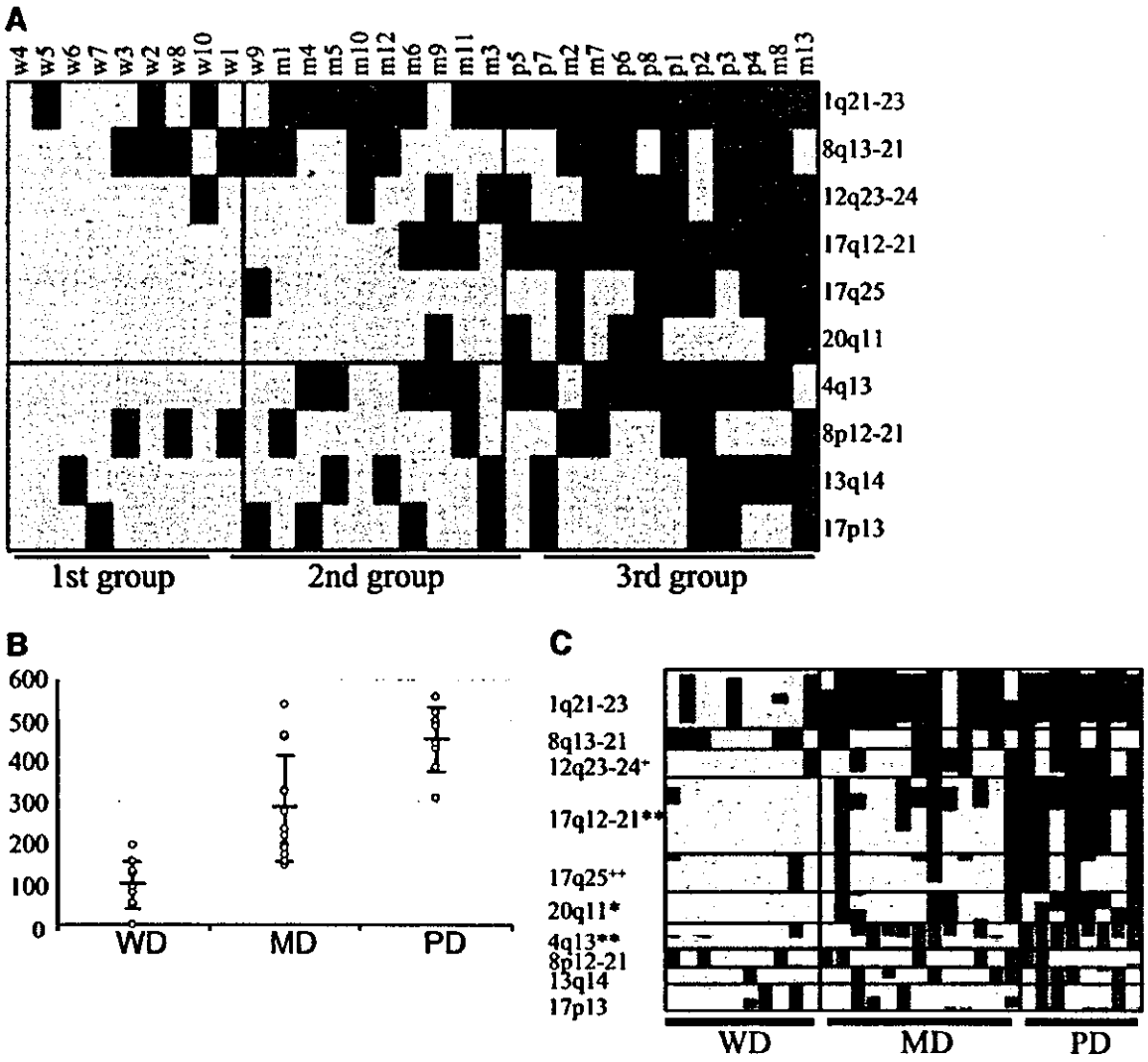

Fig. 2. Chromosomal bias of gene expression in liver cancer progression. *A*. Of 10 chromosomal regions selected by the expression imbalance map, the positive chromosomal regions were counted, and three groups were defined according to the sum of positive regions. Each column represents tissue samples and each row chromosomal regions. Relative expression levels in each chromosomal region are shown in *red* (high levels) and *blue* (low levels). *B*, chromosomal alteration in each tumor differentiation grade. Total amount of chromosomal alteration in 10 positive chromosomal regions by the expression imbalance map is increased as liver cancer develops. *Y* axis represents the total length of positive regions by the expression imbalance map (×100 kb). *C*, This analysis was carried out using 10 chromosomal regions selected by the expression imbalance map. Chromosomal change associated with each 100 kb is scored, and samples arranged according to the tumor differentiation grade. Each column represents tissue samples and each row chromosomal regions. Relative expression levels in each chromosomal region are shown in *red* (high) and *blue* (low). Statistical significance is considered as $P < 0.05$ by Mann-Whitney *U* test and shown on the left [*, statistical significance between well differentiated (WD) and moderately differentiated (MD); **, statistical significance in each differentiation grade of liver cancer; +, statistical significance between WD and MD + poorly differentiated (PD); ++, statistical significance between WD+MD and PD). Statistical significance is considered as $P < 0.05$.

genomic imbalance, we confirmed genomic aberration on chromosomes 1q21-23 and 17p13 using genomic qPCR. Specifically, all underexpressed regions 4q, 8p, 13q, and 17p have been identified by comprehensive allelotyping study (29–32), indicating that the regions with expression loss detected by expression imbalance map may be the result of loss of heterozygosity. In addition to the regions detected in previous CGH studies, we identified an expression gain in expression imbalance map at 12q23-24. The fact that 12q23-24 was identified only by the expression imbalance map and was not detected by both conventional methods and our data using qPCR suggests that there is no amplification of genome dosage but, rather, a transcriptional regulation because nine genes on 12q23-24 contain *MAZ*, *SP1*, and *E2F* binding sites in their upstream beyond expectation (data not shown). Thus, by using a new method without selective threshold processing in conjunction with a distribution-based algorithm, the expression imbalance map was able to detect regionally over- or underexpressed genes from gene expression data of oligonucleotide arrays with higher resolution than had been achieved previously (14). Furthermore, the expression imbalance map is based on microarray data and can, therefore, offer mRNA expression and expression imbalance information simultaneously.

Despite morphologic change, comprehensive expression profiling without expression imbalance map analysis fails to distinguish well differentiated from moderately differentiated.[6] In this study, using the expression imbalance map, we focused the gene alteration of differentiation grade of hepatocellular carcinoma. Expression gains of 1q21-23 and 8q13-21 and losses of 8p12-21 and 17p13 were observed in carcinogenesis from chronic liver disease to well differentiated, whereas up-regulation of 12q23-24, 17q12-21, 17q25, and 20q11 and a down-regulation of 4q13 were found only in moderately differentiated and poorly differentiated, although others reported that loss of 4q region occurred in various steps, *e.g.*, in the step from adenoma to well differentiated (33) or from well differentiated to moderately

[6] Unpublished observations.

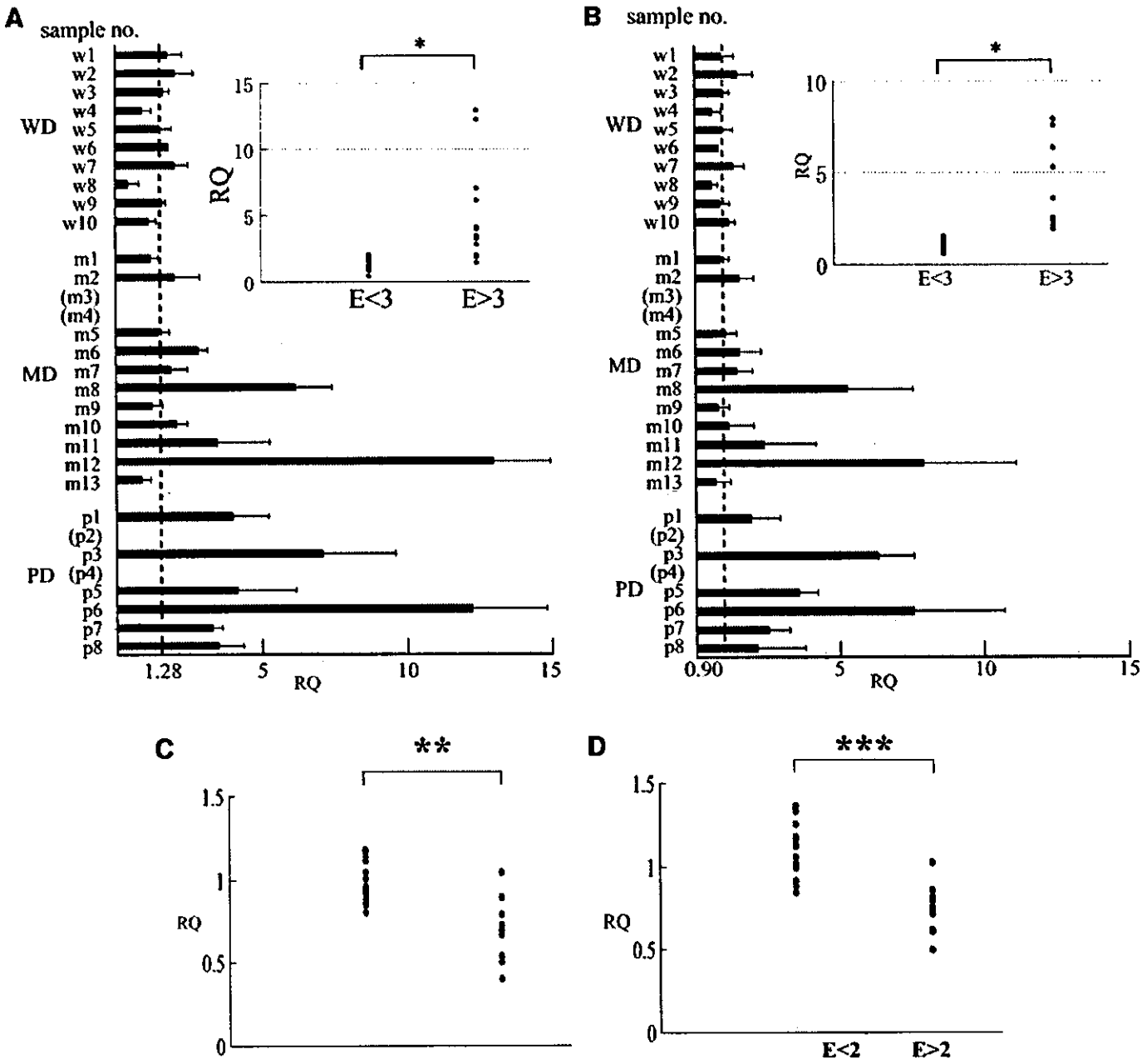

Fig. 3. Genomic imbalance of chromosome by qPCR. Genomic imbalance of chromosome 1q21-23 verified by qPCR applied to detecting copy number for liver cancer, according to differentiation grade. Amplification plots were obtained for *CCT3* and *PSMB4*, both of which were part of a highly expressed region identified by the expression imbalance map. Data are expressed as relative quantification (RQ) defined in Materials and Methods and are the mean ± SD of three determinations per experiment from three separate experiments. The *broken line* indicates the average of genome dosage of nondiseased area of livers (1.28 for *CCT3* and 0.90 for *PSMB4*). Genome dosage was compared between the two groups, an E value is <3, and >3 in the expression imbalance map, using the Mann-Whitney *U* test (shown in the top right side). (*, statistical significance was considered as $P < 0.05$). *A* in *CCT3* and *B* in *PSMB4*. Genome dosage was also compared between the two groups, an E value is <2 and >2 in expression imbalance map in 17p13 region. *C* in *ASGR1* and *D* in *DKFZP566H073*. (**, $P < 0.001$ and ***, $P < 0.0001$). Samples m3, m4, p2, and p4 were not determined because of lack of frozen specimens.

differentiated and poorly differentiated (34). These observations suggest that, including 17q12-21, which exhibits an imbalance of expression in each differentiation grade, chromosomal aberration of 4q, 12q, 17q12-21, 17q25, and 20q may play pivotal role in liver cancer progression. Our results further suggest that 1q, 8p, 8q, and 17p may be associated with initiation of hepatocarcinogenesis. Besides the chromosomal regions concerning in liver cancer progression described above, our data showed 13q14 region was concentrated on moderately differentiated and poorly differentiated, although there has no statistical significance ($P = 0.1652$), consistent with the previous reports by CGH or allelotype study (26, 34). In addition, Wilkens *et al.* (33) demonstrated that gains of 1q, 8q, and 16p and losses of 4q, 8p, and 17p were found in hepatocarcinogenesis, which were compatible to our data except for 4q and 16p. These results demonstrate a stepwise expression change in chromosomal loci correlating with hepatocellular carcinoma progression.

On 1q21-23, we focused on four growth-related genes: *HAX-1*, *SHC1*, *CKS1B*, and *CCT3*. *HAX-1* and *SHC1* have been demonstrated to induce activation of tyrosine kinases (35, 36), whereas *CKS1B* and *CCT3* may accelerate the cell cycle (37, 38). These expression gains of tyrosine kinase and cell cycle-related genes are consistent with the less differentiated, rapidly growing, liver cancer. Apart from 1q21-23, several genes that may be associated with liver cancer progression are clustered on 17q12-21 and 17q25. *AATF*, which interferes with the

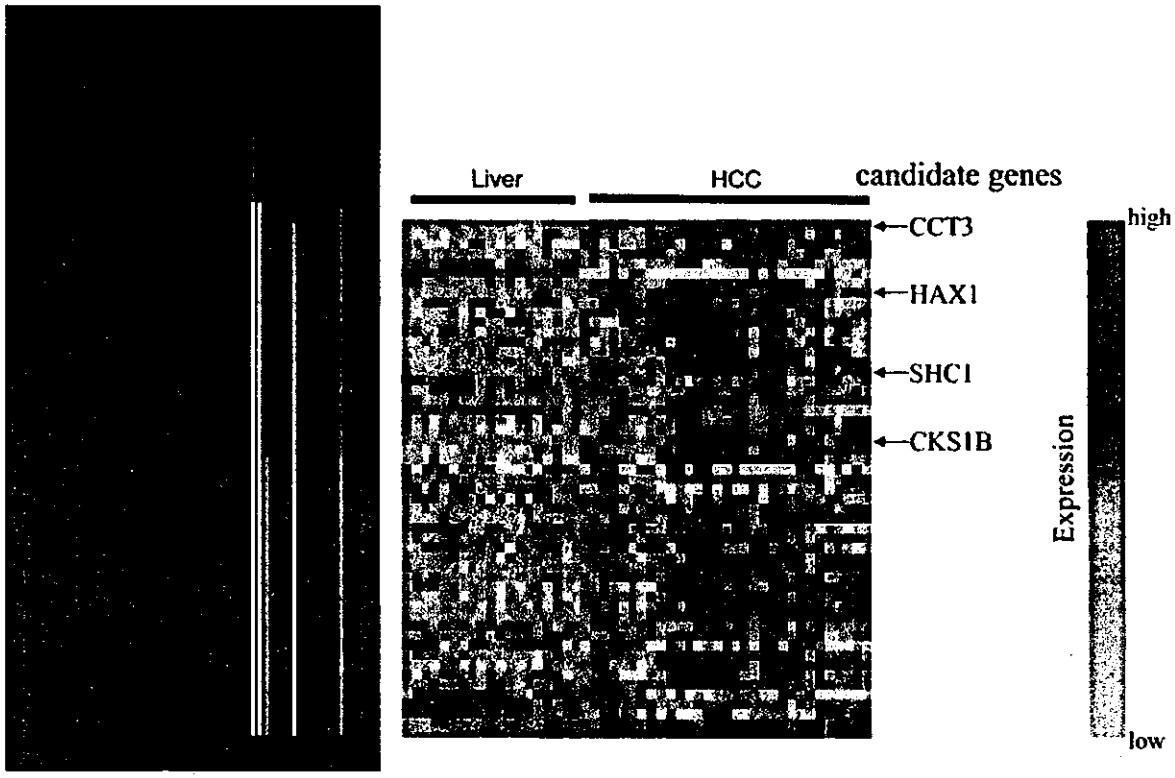

Fig. 4. Representative candidate genes responsible for liver cancer development in 1q21-23. The expression imbalance region at E value > 2 and range of an expression gain > 3.0 Mb in 1q21-23. The heat map shows relative expression levels of genes contained in the 1q21-23 region. Each column represents samples, and each row represents genes. The symbol of each candidate genes is shown on the right. Relative expression levels are shown in *red* (high) and *blue* (low).

induction of cell apoptosis through MAP3K/DLK (39), and *TK1*, a marker for the development for breast cancer (40), were also up-regulated in liver cancer.

We focused on expression change with chromosomal bias using the expression imbalance map, a recently developed method for the detection of mRNA expression imbalance regions. Comparison of expression imbalance map data with previous analysis of chromosomal imbalance identified by CGH and validation using qPCR indicate that gene expression profiles reflect chromosomal alteration. Furthermore, the expression imbalance map provides a direct measure of mRNA expression gain or loss that eliminates the need for confirmation of transcription levels of each gene. This method has the advantage that chromosomal bias and gene expression can be observed simultaneously with ease and reliability.

ACKNOWLEDGMENTS

We thank Hiroko Meguro and Aya Nonaka for valuable technical assistance, Shogo Yamamoto for excellent technical assistance and Yoshitaka Hippo for helpful discussion.

REFERENCES

1. Vogelstein B, Fearon ER, Hamilton SR, et al. Genetic alterations during colorectal-tumor development. N Engl J Med 1988;319:525–32.
2. Midorikawa Y, Tsutsumi S, Taniguchi H, et al. Identification of genes associated with dedifferentiation of hepatocellular carcinoma with expression profiling analysis. Jpn J Cancer Res 2002;93:636–43.
3. Chuma M, Sakamoto M, Yamazaki K, et al. Expression profiling in multistage hepatocarcinogenesis: identification of HSP70 as a molecular marker of early hepatocellular carcinoma. Hepatology 2003;37:198–207.
4. Kallioniemi A, Kallioniemi OP, Sudar D, et al. Comparative genomic hybridization for molecular cytogenetic analysis of solid tumors. Science (Wash. DC) 1992;258: 818–21.
5. Pollack JR, Perou CM, Alizadeh AA, et al. Genome-wide analysis of DNA copy-number changes using cDNA microarrays. Nat Genet 1999;23:41–6.
6. Pinkel D, Segraves R, Sudar D, et al. High resolution analysis of DNA copy number variation using comparative genomic hybridization to microarrays. Nat Genet 1998; 20:207–11.
7. Cai WW, Mao JH, Chow CW, Damani S, Balmain A, Bradley A. Genome-wide detection of chromosomal imbalances in tumors using BAC microarrays. Nat Biotechnol 2002;20:393–6.
8. DeRisi J, Penland L, Brown PO, et al. Use of a cDNA microarray to analyse gene expression patterns in human cancer. Nat Genet 1996;14:457–60.
9. Golub TR, Slonim DK, Tamayo P, et al. Molecular classification of cancer: class discovery and class prediction by gene expression monitoring. Science (Wash. DC) 1999;286:531–7.
10. Hippo Y, Taniguchi H, Tsutsumi S, et al. Global gene expression analysis of gastric cancer by oligonucleotide microarrays. Cancer Res 2002;62:233–40.
11. Tay ST, Leong SH, Yu K, et al. A combined comparative genomic hybridization and expression microarray analysis of gastric cancer reveals novel molecular subtypes. Cancer Res 2003;63:3309–16.
12. Mukasa A, Ueki K, Matsumoto S, et al. Distinction in gene expression profiles of oligodendrogliomas with and without allelic loss of 1p. Oncogene 2002;21:3961–8.
13. Virtaneva K, Wright FA, Tanner SM, et al. Expression profiling reveals fundamental biological differences in acute myeloid leukemia with isolated trisomy 8 and normal cytogenetics. Proc Natl Acad Sci USA 2001;98:1124–9.
14. Kano M, Nishimura K, Ishikawa S, et al. Expression imbalance map: a new visualization method for detection of mRNA expression imbalance regions. Physiol Genomics 2003;13:31–46.
15. Reis PP, Rogatto SR, Kowalski LP, et al. Quantitative real-time PCR identifies a critical region of deletion on 22q13 related to prognosis in oral cancer. Oncogene 2002;21:6480–7.
16. Chang J, Kim NG, Piao Z, et al. Assessment of chromosomal losses and gains in hepatocellular carcinoma. Cancer Lett 2002;182:193–202.
17. Kitay-Cohen Y, Amiel A, Ashur Y, et al. Analysis of chromosomal aberrations in large hepatocellular carcinomas by comparative genomic hybridization. Cancer Genet Cytogenet 2001;131:60–4.
18. Niketeghad F, Decker HJ, Caselmann WH, et al. Frequent genomic imbalances suggest commonly altered tumour genes in human hepatocarcinogenesis. Br J Cancer 2001;85:697–704.
19. Shiraishi K, Okita K, Kusano N, et al. A comparison of DNA copy number changes detected by comparative genomic hybridization in malignancies of the liver, biliary tract and pancreas. Oncology 2001;60:151–61.
20. Balsara BR, Pei J, De Rienzo A, et al. Human hepatocellular carcinoma is characterized by a highly consistent pattern of genomic imbalances, including frequent loss of 16q23.1-24.1. Genes Chromosomes Cancer 2001;30:245–53.

21. Tornillo L, Carafa V, Richter J, et al. Marked genetic similarities between hepatitis B virus-positive and hepatitis C virus-positive hepatocellular carcinomas. J Pathol 2000;192:307–12.
22. Wong N, Lai P, Pang E, et al. Genomic aberrations in human hepatocellular carcinomas of differing etiologies. Clin Cancer Res 2000;6:4000–9.
23. Guan XY, Fang Y, Sham JS, et al. Recurrent chromosome alterations in hepatocellular carcinoma detected by comparative genomic hybridization. Genes Chromosomes Cancer 2000;29:110–6.
24. Marchio A, Pineau P, Meddeb M, et al. Distinct chromosomal abnormality pattern in primary liver cancer of non-B, non-C patients. Oncogene 2000;19:3733–8.
25. Sakakura C, Hagiwara A, Taniguchi H, et al. Chromosomal aberrations in human hepatocellular carcinomas associated with hepatitis C virus infection detected by comparative genomic hybridization. Br J Cancer 1999;80:2034–9.
26. Kusano N, Shiraishi K, Kubo K, Oga A, Okita K, Sasaki K. Genetic aberrations detected by comparative genomic hybridization in hepatocellular carcinomas: their relationship to clinicopathological features. Hepatology 1999;29:1858–62.
27. Marchio A, Meddeb M, Pineau P, et al. Recurrent chromosomal abnormalities in hepatocellular carcinoma detected by comparative genomic hybridization. Genes Chromosomes Cancer 1997;18:59–65.
28. Wong N, Lai P, Lee SW, et al. Assessment of genetic changes in hepatocellular carcinoma by comparative genomic hybridization analysis: relationship to disease stage, tumor size, and cirrhosis. Am J Pathol. 1999;154:37–43.
29. Bluteau O, Beaudoin JC, Pasturaud P, et al. Specific association between alcohol intake, high grade of differentiation and 4q34–q35 deletions in hepatocellular carcinomas identified by high resolution allelotyping. Oncogene 2002;21:1225–32.
30. Nishimura T, Nishida N, Itoh T, et al. Comprehensive allelotyping of well-differentiated human hepatocellular carcinoma with semiquantitative determination of chromosomal gain or loss. Genes Chromosomes Cancer 2002;35:329–39.
31. Chan KL, Lee JM, Guan XY, Fan ST, Ng IO. High-density allelotyping of chromosome 8p in hepatocellular carcinoma and clinicopathologic correlation. Cancer (Phila.) 2002;94:3179–85.
32. Wong CM, Lee JM, Lau TC, Fan ST, Ng IO. Clinicopathological significance of loss of heterozygosity on chromosome 13q in hepatocellular carcinoma. Clin Cancer Res 2002;8:2266–72.
33. Wilkens L, Bredt M, Flemming P, Becker T, Klempnauer J, Kreipe HH. Differentiation of liver cell adenomas from well-differentiated hepatocellular carcinomas by comparative genomic hybridization. J Pathol 2001;193:476–82.
34. Okabe H, Ikai I, Matsuo K, et al. Comprehensive allelotype study of hepatocellular carcinoma: potential differences in pathways to hepatocellular carcinoma between hepatitis B virus-positive and -negative tumors. Hepatology 2000;31:1073–9.
35. Suzuki Y, Demoliere C, Kitamura D, Takeshita H, Deuschle U, Watanabe T. HAX-1, a novel intracellular protein, localized on mitochondria, directly associates with HS1, a substrate of Src family tyrosine kinases. J Immunol 1997;158:2736–44.
36. McGlade J, Cheng A, Pelicci G, Pelicci PG, Pawson T. Shc proteins are phosphorylated and regulated by the v-Src and v-Fps protein-tyrosine kinases. Proc Natl Acad Sci USA 1992;89:8869–73.
37. Ganoth D, Bornstein G, Ko TK, et al. The cell-cycle regulatory protein Cks1 is required for SCF(Skp2)-mediated ubiquitinylation of p27. Nat Cell Biol 2001;3:321–4.
38. Won KA, Schumacher RJ, Farr GW, Horwich AL, Reed SI. Maturation of human cyclin E requires the function of eukaryotic chaperonin CCT. Mol Cell Biol 1998;18:7584–9.
39. Page G, Lodige I, Kogel D, Scheidtmann KH. AATF, a novel transcription factor that interacts with Dlk/ZIP kinase and interferes with apoptosis. FEBS Lett 1999;462:187–91.
40. O'Neill KL, Hoper M, Odling-Smee GW. Can thymidine kinase levels in breast tumors predict disease recurrence? J Natl Cancer Inst (Bethesda) 1992;84:1825–8.

[CANCER RESEARCH 64, 2418–2423, April 1, 2004]

Identification of Soluble NH_2-Terminal Fragment of Glypican-3 as a Serological Marker for Early-Stage Hepatocellular Carcinoma

Yoshitaka Hippo,[1] Kiyotaka Watanabe,[4] Akira Watanabe,[1] Yutaka Midorikawa,[5] Shogo Yamamoto,[2] Sigeo Ihara,[2] Susumu Tokita,[7] Hiroko Iwanari,[7] Yukio Ito,[7] Kiyotaka Nakano,[6] Jun-ichi Nezu,[6] Hiroyuki Tsunoda,[6] Takeshi Yoshino,[6] Iwao Ohizumi,[6] Masayuki Tsuchiya,[6] Shin Ohnishi,[4] Masatoshi Makuuchi,[5] Takao Hamakubo,[3] Tatsuhiko Kodama,[3] and Hiroyuki Aburatani[1]

[1]Genome Science Division, [2]Division of Dynamical Bioinformatics, and [3]Division of Molecular Biology and Medicine, Research Center for Advanced Science and Technology, The University of Tokyo, Tokyo, Japan; Departments of [4]Gastroenterology and [5]Hepato-Biliary-Pancreatic Surgery, Graduate School of Medicine, The University of Tokyo, Tokyo, Japan; [6]Chugai Pharmaceutical Co., Ltd., Shizuoka, Japan; and [7]Perseus Proteomics, Inc., Tokyo, Japan

ABSTRACT

For detection of hepatocellular carcinoma (HCC) in patients with liver cirrhosis, serum α-fetoprotein has been widely used, but its sensitivity has not been satisfactory, especially in small, well-differentiated HCC, and complementary serum marker has been clinically required. Glypican-3 (GPC3), a heparan sulfate proteoglycan anchored to the plasma membrane, is a good candidate marker of HCC because it is an oncofetal protein overexpressed in HCC at both the mRNA and protein levels. In this study, we demonstrated that its NH_2-terminal portion [soluble GPC3 (sGPC3)] is cleaved between Arg^{358} and Ser^{359} of GPC3 and that sGPC3 can be specifically detected in the sera of patients with HCC. Serum levels of sGPC3 were 4.84 ± 8.91 ng/ml in HCC, significantly higher than the levels seen in liver cirrhosis (1.09 ± 0.74 ng/ml; $P < 0.01$) and healthy controls (0.65 ± 0.32 ng/ml; $P < 0.001$). In well- or moderately-differentiated HCC, sGPC3 was superior to α-fetoprotein in sensitivity, and a combination measurement of both markers improved overall sensitivity from 50% to 72%. These results indicate that sGPC3 is a novel serological marker essential for the early detection of HCC.

INTRODUCTION

Hepatocellular carcinoma (HCC) is one of the most prevalent cancers worldwide, and its incidence is still increasing (1). Because HCC develops from cirrhotic liver after chronic infection with hepatitis virus B or C, patients with liver cirrhosis (LC) are advised to undergo periodical screening of serum α-fetoprotein (AFP) levels and liver ultrasound for the purpose of early detection of cancer (2). AFP is a glycoprotein expressed abundantly in fetal liver but not in normal adult liver and is re-expressed by HCC as it dedifferentiates from a premalignant lesion in the cirrhotic liver through well-differentiated (WD) and moderately differentiated (MD) HCC to poorly differentiated HCC (3). AFP has been used as a serum marker of HCC for more than 40 years. However, ultrasound imaging has been more effective lately in early detection of small WD HCC, in which AFP has yet to be elevated (4), highlighting the clinical need for novel sensitive serum markers for WD HCC.

Many previous studies have identified genes up-regulated in HCC compared with surrounding noncancerous lesions using differential display or cDNA subtraction (5–8). Recently, microarray studies on HCC presented gene lists containing a number of overexpressed genes (9–14). However, to determine whether a gene is a good candidate as a serological marker of WD HCC, it is crucial to determine the following: (*a*) whether it is overexpressed in WD HCC; (*b*) whether it is not expressed abundantly in other normal organs; and (*c*) whether it is detectable in the serum.

Overexpression of *GPC3* mRNA in HCC has been reported by ourselves and several other groups (15–18). Moreover, frequency of *GPC3* mRNA overexpression was significantly higher than that of elevated serum level and mRNA level of AFP in small HCC (16). We also observed frequent overexpression of *GPC3* in WD HCC compared with AFP with microarray analysis.[8] Together with minimal expression in normal organs (16, 19), GPC3 has, undoubtedly, previously existed as an attractive candidate marker of HCC. We showed previously using a monoclonal antibody (mAb) that GPC3 protein is also highly expressed in HCC (15). In this study, we further characterized GPC3 protein using a panel of newly generated mAbs and investigated whether it could be detected specifically in the sera of the patients with HCC. Finally, we successfully established a detection system for the soluble fragment of GPC3 (sGPC3) and confirmed its usefulness as a novel biomarker for HCC.

MATERIALS AND METHODS

Serum Samples. Serum samples were collected at Tokyo University Hospital with informed consent from 69 patients with HCC and 38 patients with LC, defined according to the following criteria: patients with a pathological diagnosis of HCC after surgery or with evidence of tumor stain on computed tomography or angiography were diagnosed with HCC; and patients diagnosed with LC were limited to those who had no history of HCC and no ultrasound evidence of tumor for more than 6 months from the day of serum collection.

Purification of Recombinant GPC3 Proteins. For protein expression, we used modified pCXN vector that contained dihydrofolate reductase expression unit as a selection marker. Original pCXN vector (20) was generously provided by J. Miyazaki (Osaka University Medical School, Osaka, Japan). An expression vector for GPC3 that lacks the COOH-terminal hydrophobic glycosylated phosphatidylinositol (GPI)-anchoring domain, GPC3ΔGPI, was constructed by introducing cDNA corresponding to amino acid residues 1–563 of GPC3 into modified pCXN with a FLAG tag added at the COOH terminus. An expression vector for GPC3ΔGPI without heparan sulfate, GPC3ΔGPIΔHS, was constructed by changing Ser^{495} and Ser^{509} to Ala to abolish the heparan sulfate attachment site. These constructs were stably transfected into Chinese hamster ovary cells deficient in the dihydrofolate reductase gene. Culture media containing GPC3ΔGPI-FLAG or GPC3ΔGPIΔHS-FLAG recombinant proteins were collected and loaded to DEAE ion-exchange chromatography DEAE Sepharose FF (Amersham Bioscience, Tokyo, Japan). After washing, eluted protein solutions were applied to anti-FLAG M2 antibody beads (Sigma, St.

Received 7/19/03; revised 11/25/03; accepted 1/12/04.

Grant support: Grants-in-Aid for Scientific Research (B) 12557051 and 13218019 and Scientific Research on Priority Areas (C) 12217031 from the Ministry of Education, Culture, Sports, Science and Technology; Health and Labor Sciences Research Grants for Research on Hepatitis and BSE from the Ministry of Health Labor and Welfare; and funds from Uehara Memorial Foundation (H. Aburatani). This study was carried out as a part of The Technology Development for Analysis of Protein Expression and Interaction in Bioconsortia on R&D of New Industrial Science and Technology Frontiers that was overseen by the Industrial Science, Technology and Environmental Policy Bureau, Ministry of Economy, Trade and Industry and delegated to New Energy Development Organization.

The costs of publication of this article were defrayed in part by the payment of page charges. This article must therefore be hereby marked *advertisement* in accordance with 18 U.S.C. Section 1734 solely to indicate this fact.

Requests for reprints: Hiroyuki Aburatani, Genome Science Division, Research Center for Advanced Science and Technology, The University of Tokyo, 4-6-1 Komaba, Meguro-ku, Tokyo 153-8904, Japan. Phone: 81-3-5452-5235; Fax: 81-3-5452-5355; E-mail: haburata-tky@umin.ac.jp.

[8] Y. Midorikawa, S. Tsutsumi, K. Nishimura, N. Kamimura, M. Kano, H, Sakamoto, M. Makuuchi, and H. Aburatani. Transcriptional Signature in Progression of Hepatocellular Carcinoma, manuscript in preparation.

Louis, MO). Proteins eluted with solution containing 200 μg/ml FLAG peptide (Sigma) were subjected to gel filtration chromatography with HiLoad 26/60 Superdex200pg (Amersham Bioscience). Finally, recombinant protein was concentrated using DEAE Sepharose FF.

Generation of Anti-GPC3 mAbs. We used recombinant GPC3ΔGPI as an immunogen. Spleen cells were isolated and fused with mouse myeloma P3-X63Ag8U1 cells (American Type Culture Collection, Manassas, VA). Hybridomas were selected by ELISA against the purified recombinant GPC3ΔGPIΔHS-FLAG, followed by cloning with limited dilution. Three mouse mAbs (A1836A, M18D04, and M19B11) were used in this study. For epitope mapping of these mAbs, a pGEX-5X (Amersham Biosciences) construct for the NH_2-terminal portion of GPC3 (amino acids 25–358) was expressed in *Escherichia coli* BL21 Codon Plus (DE3) pLys (Stratagene, La Jolla, CA) as a glutathione *S*-transferase-fusion protein and subject to immunoblotting analysis.

Immunoblotting. Total cell lysates were obtained after lysis in 10 mM Tris (pH 7.4), 150 mM NaCl, 5 mM EDTA, 1.0% Triton X-100, 1.0% sodium deoxycholate, and 0.1% SDS with protease inhibitor mixture (Sigma). Culture supernatant was obtained from serum-free medium used for culture of hepatoma cells. Proteins were separated with 12% SDS-PAGE and transferred to polyvinylidene difluoride Hybond P membrane (Amersham Biosciences). The membrane was treated with 2% nonfat milk in TBS containing 0.05% Tween 20 (TBST) followed by incubation with anti-GPC3 mAb in TBST and subsequent incubation with horseradish peroxidase-conjugated secondary antibody (dilution, 1:5000; Amersham Biosciences) in TBST. The protein was visualized using the enhanced chemiluminescence plus detection system (Amersham Biosciences).

Immunoprecipitation. We first prepared antibody beads by covalently linking 25 μl of protein G-Sepharose (Amersham Biosciences) and 50 μg of anti-GPC3 mAb M18D04 or M19B11 with 20 mM dimethyl pimelimidate (ICN Aurora, Aurora, OH). We then added 50 μl of sera from the patients or culture media of HuH7 cells diluted in 250 μl with PBS to 25 μl of antibody beads and incubated them for 2 h at 4°C. After extensive washing with PBS, antibody beads were boiled for 5 min in 50 μl of SDS-PAGE loading buffer containing 10% 2-mercaptoethanol, and subsequently, immunoblotting was performed.

Sandwich ELISA. One μg of anti-GPC3 mAb A1836A per well was immobilized to 96-well plate Maxisorp (Nalge Nunc International, Roskilde, Denmark) and stabilized with Immunoassay Stabilizer (Advanced Biotechnologies Inc., Columbia, MD). Twenty-five μl of sera or standard were diluted with 100 μl of buffer containing 20% normal rabbit serum (Pel-Freez Biologicals, Rogers, AR), 1% BSA (Oriental Yeast Co., Ltd., Osaka, Japan), and 2% mouse ascites Hyb-3423 (Institute of Immunology, Tokyo, Japan) in 50 mM Tris-Cl (pH 8.0), 0.15 M NaCl, and 1 mM EDTA and incubated at room temperature for 2 h. After washing, 25 μl of biotinylated antibody solution containing anti-GPC3 mAbs M18D04 (1.88 μg/ml) and M19B11 (3.75 μg/ml) and 100 μl of horseradish peroxidase-labeled streptavidin (Vector Laboratories Inc., Burlingame, CA) were added to the plate and incubated twice at room temperature for 30 min. TMB Soluble Reagent and Stop Buffer (Scy Tek Laboratories, Inc., Logan, UT) were added as substrate, and absorbance at 450 nm was read with EIA Reader (Corona Electric Co., Ltd., Ibaraki, Japan). Recombinant GPC3ΔGPI was used as a standard sample in each assay.

Amino Acid Sequence Analysis. Recombinant GPC3ΔGPI and GPC3ΔGPIΔHS were purified and separated by SDS-PAGE and transferred to polyvinylidene difluoride membrane ProBlott (Applied Biosystems, Foster City, CA). The membrane was stained with CBB R-250, and sections containing bands of M_r 40,000 and M_r 30,000 were cut out separately. These polyvinylidene difluoride membrane sections were washed with a solution including 50% acetonitrile and 0.1% trifluoroacetic acid and applied to an ABI 492 Protein Sequencer (Applied Biosystems) to sequence the NH_2 terminus of the protein. Because the NH_2 terminus of the M_r 40,000 protein was blocked, the membrane was further incubated in acetate with 0.6 mg/ml 3-bromo-3-methyl-2-nitrophenyl-mecapto-3*H*-indole (ICN Biomedicals Inc., Irvine, CA) at 80°C for 1 h in the dark to chemically cleave the protein at the COOH terminus of tryptophan residues. After washing twice with 80% acetate and once with 10% methanol, the peptide was analyzed using an ABI 492 Protein Sequencer. The detected sequence was aligned using FASTS software available online,[9] and the protein was identified.

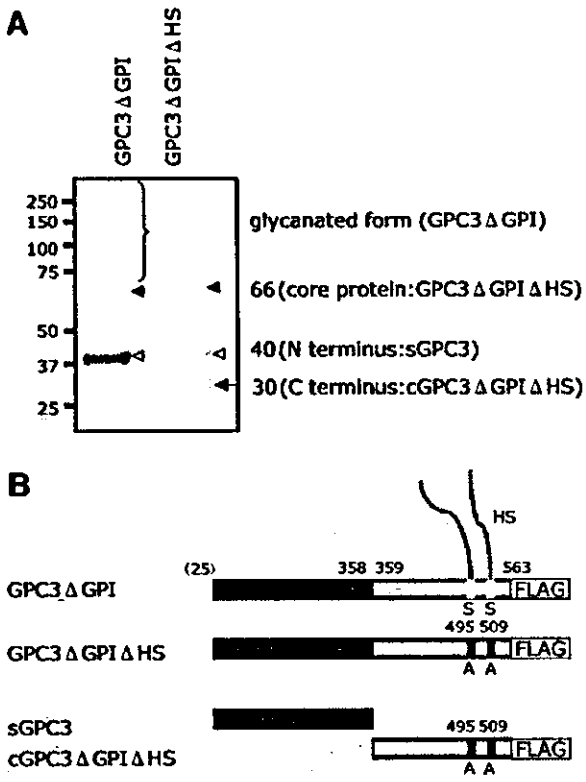

Fig. 1. Characterization of recombinant glypican-3 (GPC3) proteins. *A*, CBB R-250-stained SDS-PAGE of purified recombinant GPC3. *Brace*, glycanated GPC3 (smearing), GPC3ΔGPI; *closed arrowhead*, core protein of GPC3 (M_r 66,000) that lacks heparan sulfate glycosaminoglycan, GPC3ΔGPIΔHS; *open arrowhead*, sGPC3 (M_r 40,000); *arrow*, cGPC3ΔGPIΔHS (M_r 30,000). *B*, schematic diagram of recombinant proteins. *Numbers above the boxes* indicate amino acid residue number. Note that NH_2-terminal residue 25 is putative and indicated in *parentheses*. *HS*, heparan sulfate glycosaminoglican.

RESULTS

The NH_2-Terminal Portion of GPC3 Is Cleaved between Arg^{358} and Ser^{359} *in Vitro*. We have previously generated mAb K6534 raised against a peptide corresponding to amino acids 355–371 of GPC3 protein, and we demonstrated, for the first time, overexpression of its core protein in HCC with immunoblotting using this antibody (15). Another antibody is required to construct a sandwich ELISA system for serum examination of GPC3, so we started generating high-affinity mAbs using recombinant GPC3ΔGPI as an immunogen. While purifying the immunogen from the culture supernatant of Chinese hamster ovary cells, we observed a M_r 40,000 band (Fig. 1*A*) in addition to the M_r 66,000 band that corresponds to core protein of GPC3 as observed with K6534 (15).

Because the NH_2 terminus of this M_r 40,000 band was modified, as revealed by initial amino acid sequencing, we performed sequencing of internal amino acids of the band after cleavage at the COOH terminus of tryptophan residues to verify its origin. We detected six cycles of three amino acid residues VRY, EPX, YES, ITY, LPX, and QSV, each cycle corresponding to the first to sixth residue following tryptophan (W), respectively. After alignment with FASTF algorithm, these sequences matched with the (W)VPETPV (amino acid 51–57), (W)YCSYCQ (amino acid 261–267), and (W)REYILS (amino acid

[9] http://fasta.bioch.virginia.edu/.

296–302) partial sequences of GPC3, respectively, indicating that this band is derived from an NH_2-terminal portion of GPC3. We designated this soluble cleaved fragment of GPC3 as sGPC3.

To further characterize sGPC3, we next tried to precisely identify the undetermined cleavage site by sequencing the residual COOH-terminal portion of GPC3 (designated cGPC3). However, the corresponding band was not visible by SDS-PAGE, presumably due to attachment of heparan sulfate glycosaminoglycan, leading to smearing (Fig. 1*A*). After substituting the two heparan sulfate attachment sites of the expression construct and purifying the resultant GPC3ΔGPIΔHS, we could observe a band of M_r 30,000, as expected (Fig. 1*A*). The NH_2-terminal sequence of this band was identified as SAYYPEDLF, identical to amino acids 359–367 of GPC3. Thus, the cleavage site was identified as being between Arg^{358} and Ser^{359} (Fig. 1*B*). We do not have precise information on the NH_2-terminal sequence of sGPC3 due to modification, but considering that amino acid 1–24 is a putative signal sequence, sGPC3 is likely to consist of amino acids 25–358 with an estimated molecular weight of 38,100, consistent with the M_r 40,000 band observed in SDS-PAGE (Fig. 1*A*).

Soluble GPC3 Is a Major Form of GPC3 Specifically Detected in the Sera of Patients with HCC. We succeeded in generating a number of high-affinity mAbs specific for GPC3 and classified these antibodies into two groups, N-mAbs and C-mAbs, according to their epitopes within amino acids 25–358 or 359–563, respectively (data not shown). These antibodies could also recognize endogenous GPC3 protein in immunoblotting: core protein (M_r 66,000) and glycanated form (smearing) of GPC3 were detected by both N-mAbs and C-mAbs; whereas sGPC3 (M_r 40,000) was detected only by N-mAbs (Fig. 2*A*). An additional M_r 50,000 band was detected strongly in the cell lysate of HepG2 with both N-mAbs and C-mAbs (Fig. 2*A*). This band was only weakly detectable in HuH6 cells and was undetectable in five other hepatoma cell lines (Fig. 2, *A* and *C*; data not shown), suggesting cell-specific variations in the processing of the protein. In the culture supernatant, sGPC3, rather than a core protein or a glycanated form of GPC3, was the major form of GPC3 detected (Fig. 2*A*).

Based on the above *in vitro* finding, we speculated that sGPC3, instead of core protein of GPC3, might be the major form of GPC3 in the sera of HCC patients. To avoid possible interference on immunoblotting by significant migration of albumin or immunoglobulin in the serum, we performed immunoprecipitation before immunoblottng using three N-mAbs (Fig. 2*B*). sGPC3 alone was successfully detected by immunoprecipitation with M18D04 (Fig. 2*C*) or M19B11 (data not shown) followed by immunoblotting with A1836A in the sera of patients with HCC, but not in sera from normal liver (NL). These results clearly demonstrate that sGPC3 is the major diagnostic target specifically detectable in the sera of HCC patients.

Soluble GPC3 Is Useful as a Serological Marker of WD HCC and MD HCC. We next constructed a sandwich ELISA system with these three antibodies to measure the serum level of sGPC3 (Fig. 3*A*). To verify the specificity of the assay, we performed immunoblotting of 10 sera samples from HCC with sGPC3 levels ranging from 4.0 to 55.0 ng/ml and 3 samples from NL with sGPC3 levels of <0.1 mg/ml. We detected only sGPC3 in all 10 HCC samples, whereas no band was detected in 3 samples from NL, indicating high sensitivity and specificity of the assay (Fig. 3*B*). When we examined sera from 69 cases with HCC, 38 cases with LC, and 96 cases with NL, the level of sGPC3 (mean ± SD) was 4.84 ± 8.91 ng/ml for HCC, 1.09 ± 0.74 ng/ml for LC, and 0.65 ± 0.32 ng/ml for NL and was significantly higher in HCC than in NL ($P < 0.001$, Student's t test) or in LC ($P < 0.01$; Fig. 3*C*).

We then evaluated sGPC3 as a general marker for HCC in comparison with AFP. Initial analysis of the receiver-operating characteristic curve using the data from 69 cases with HCC and 38 cases with LC suggested that, used in isolation, sGPC3 is not as good as AFP: the calculated area under the receiver-operating characteristic curve was 0.729 for sGPC3 and 0.799 for AFP (Fig. 3*D*). The sensitivity and specificity of sGPC3 for the diagnosis of HCC (cutoff value, 2.0 ng/ml) were 51% and 90%, respectively, whereas those of AFP measured in parallel (cutoff value, 20 ng/ml) were 55% and 90%, respectively. AFP and sGPC3 were not correlated ($r = 0.13$), and combination measurement of both markers markedly improved sensitivity to 72%.

HCC may be divided into two subgroups correlating to the extent of disease: (*a*) one first treated by surgery, mainly with a solitary tumor or few tumors; and (*b*) the second treated with transcatheter arterial chemoembolization, mostly with multiple and advanced tumors. The serum level of sGPC3 was 2.61 ± 2.69 ng/ml for the former group,

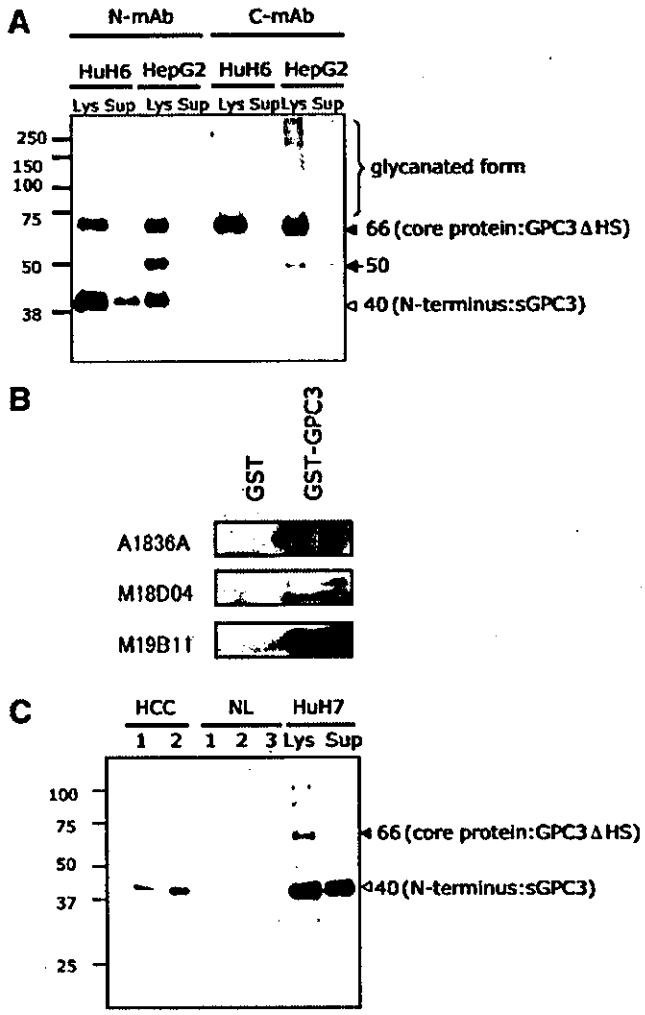

Fig. 2. Characterization of endogenous glypican-3 (GPC3) proteins with monoclonal antibodies (mAbs). *A*, representative immunoblotting of endogenous GPC3 in the cell lysate and culture supernatant with N-mAb and C-mAb. HepG2 and HuH6 were analyzed. Note that soluble GPC3 (sGPC3) alone is detected in the culture supernatant. *Brace*, glycanated GPC3 (smearing); *closed arrowhead*, core protein of GPC3 (M_r 66,000); *open arrowhead*, sGPC3 (M_r 40,000); *arrow*, uncharacterized processed fragment of GPC3 (M_r 50,000). *Lys*, lysate; *Sup*, supernatant of culture media. *B*, immunoblotting analysis with anti-GPC3 antibodies A1836A, M18D04, and M19B11 recognized glutathione *S*-transferase-sGPC3 but did not recognize glutathione *S*-transferase. *C*, detection of sGPC3 alone in the sera of the patients with hepatocellular carcinoma. Sera from two patients with hepatocellular carcinoma and three healthy adults (NL) were analyzed by immunoprecipitation with M18D04 followed by immunoblotting with A1836A. HuH7 cells were analyzed as a reference. *Closed arrowhead*, core protein of GPC3 (M_r 66,000); *open arrowhead*, sGPC3 (M_r 40,000).

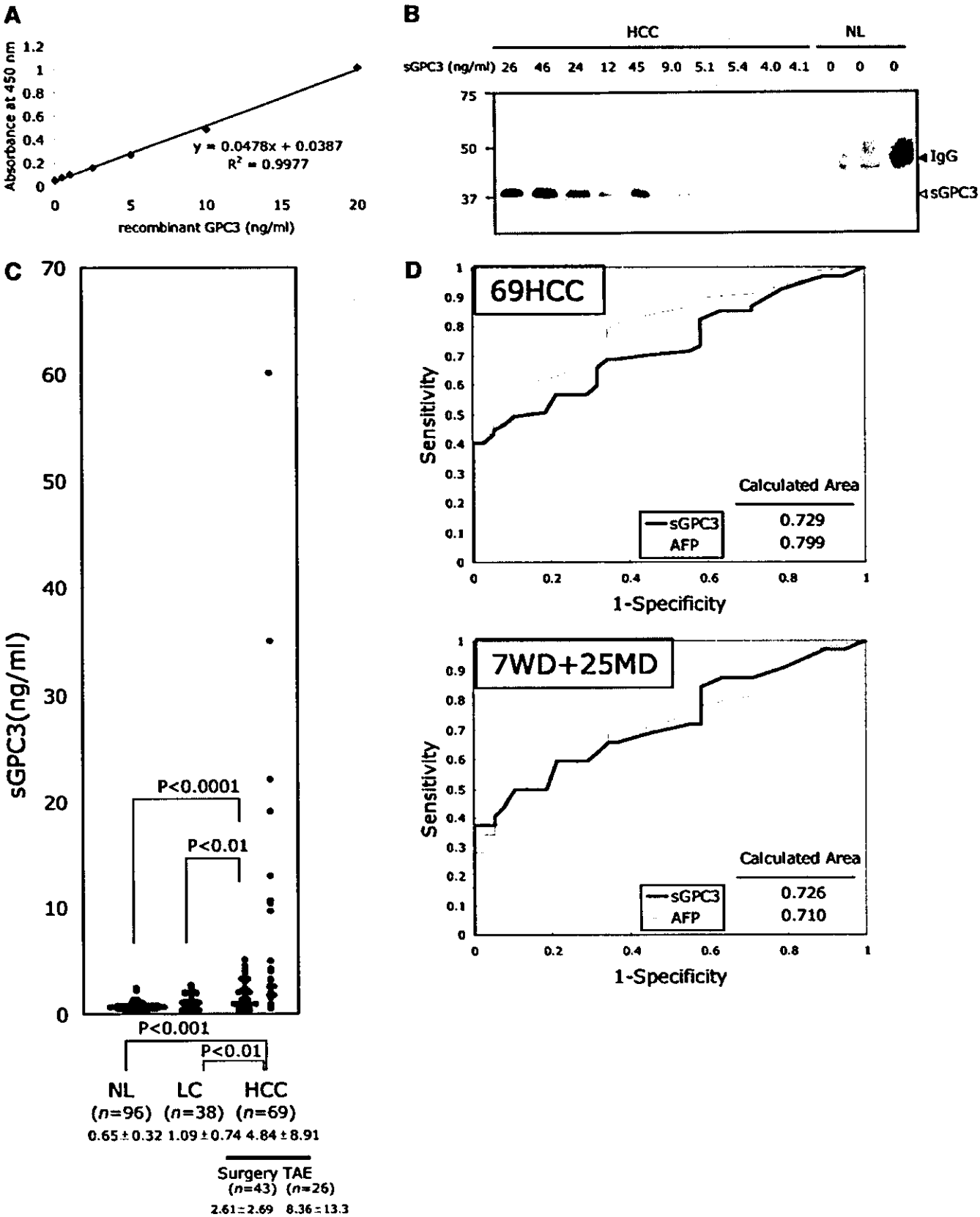

Fig. 3. Evaluation of soluble glypican-3 (sGPC3) as a serological marker of hepatocellular carcinoma (HCC). *A*, standard curve of sandwich ELISA. *B*, high specificity of sandwich ELISA. Specific detection of sGPC3 alone solely in the sera with elevated sGPC3 level measured with sandwich ELISA. Sera from 10 patients with HCC and 3 healthy adults (*NL*) were analyzed by immunoprecipitation with M18D04 followed by immunoblotting with A1836A. Serum sGPC3 level is indicated for each sample. *Open arrowhead*, sGPC3 (M_r 40,000); *closed arrowhead*, IgG. *C*, distribution of sGPC3 in the sera of patients with normal liver, liver cirrhosis (*LC*), and HCC (surgery and transcatheter arterial chemoembolization subgroup). Mean ± SD (ng/ml) of serum sGPC3 is indicated. Number of samples is indicated as *n*. *D*, receiver-operating characteristic curve analysis of sGPC3 (*thick line*) and α-fetoprotein (*thin line*). *Top panel*, all of the 69 HCCs and 38 cases of LC were included in the analysis. *Bottom panel*, 32 HCCs (including 7 well-differentiated and 25 moderately differentiated HCCs) and 38 cases of LC were analyzed. Area under the receiver-operating characteristic curve is indicated.

significantly higher than that for NL ($P < 0.0001$, Student's t test) or LC ($P < 0.01$), and 8.36 ± 13.3 ng/ml for the latter group (Fig. 3*C*), suggesting that the serum level of sGPC3 is elevated in an earlier stage and rises as HCC progresses. We then evaluated sGPC3 as a marker for HCC in relatively early-stage disease. When 43 cases treated by surgery were confined to 32 cases with relatively early-stage HCC (7 cases with WD HCC and 25 cases with MD HCC), calculated areas under the receiver-operating characteristic curve for sGPC3 and AFP were 0.726 and 0.710, respectively, indicating that sGPC3 is superior to AFP (Fig. 3*D*). The sensitivity of sGPC3 and AFP for the diagnosis of WD HCC and MD HCC was 50% and 47%, respectively. Moreover, combination measurement of both markers in WD HCC and MD HCC also markedly improved sensitivity to 72%. These results clearly demonstrate the utility of sGPC3 as a serological marker for HCC, especially for relatively early-stage HCC, and its complementarity to AFP.

DISCUSSION

GPC3 (alternatively called OCI-5 or MXR-7) is a heparan sulfate proteoglycan. The structural characteristics of the glypican family are (*a*) a core protein of approximately M_r 60,000, (*b*) binding to the membrane through GPI anchor, (*c*) heparan sulfate glycosaminoglycan attachment at Ser-Gly sequence within the COOH-terminal portion, and (*d*) a highly conserved pattern of 14 Cys residues (19). *GPC3* was originally isolated as a gene that is developmentally expressed in fetal rat intestine (21, 22). Mutation of *GPC3* is found in Simpson-Golabi-Behmel syndrome characterized by an overgrowth phenotype, hence its putative function was associated with an apoptotic effect (23). Silencing of *GPC3* in some types of cancer (24–26) is in line with this notion.

Overexpression of *GPC3* mRNA in HCC has been reported by ourselves and several other groups (15–18), although the role of GPC3 in carcinogenesis or progression of HCC has yet to be determined. In general, transcription level and protein level do not necessarily correlate. We have succeeded previously in generating an anti-GPC3 mAb against a peptide within the COOH-terminal portion, and we demonstrated using the antibody that the expression level of GPC3 core protein correlated well with its transcription level and that GPC3 was also overexpressed at protein level for the first time (15). Difficulties in making high-affinity antibodies against GPC3 (27), presumably due to its complex structure derived from disulfide bonds between 14 Cys residues, prohibited further analysis. We tried to generate high-affinity mAbs again by using recombinant GPC3 protein expressed in mammalian cells as an immunogen, and we finally succeeded in generating numerous high-affinity mAbs; to our knowledge, this is the first establishment of mAbs that can react with sGPC3. We did not recognize sGPC3 in a previous study (15) because we used a mAb against a relatively COOH-terminal portion (amino acids 355–371).

In the present work, we have precisely characterized GPC3 and demonstrated that the M_r 40,000 protein, sGPC3, derives from the NH_2-terminal portion of GPC3 and is cleaved between Arg^{358} and Ser^{359}. The M_r 40,000 protein was previously described by Mast *et al.* (19), who were searching for the binding protein on the plasma membrane of HepG2 cells for tissue factor pathway inhibitor. They purified a M_r 40,000 protein from culture supernatant of HepG2 cells and showed that it was derived from the NH_2-terminal portion of GPC3. They did not identify a cleavage site for the protein, unlike our study, but it is highly likely that the soluble protein they observed is sGPC3. They described purification of a M_r 40,000 protein only when protease inhibitors were used throughout the procedure, strongly suggesting that GPC3 cleavage is mediated by a protease (19). In addition, they found that washing the cells with dextran sulfate or heparin released significantly higher amounts of GPC3 than seen before treatment, strongly suggesting that most GPC3 is noncovalently attached to the cell surface after cleavage of the GPI anchor, but not in the culture supernatant (19). Our finding that sGPC3 alone is the major form of GPC3 in the culture supernatant of hepatoma cells and the serum of patients with HCC is consistent with these findings.

Very recently, two other groups reported elevated levels of GPC3 in the serum of HCC patients. The results still seem preliminary, although they are quite similar to ours. Here, we have made significant improvements in the reliability of the assay. Nakatsura *et al.* (28) used a polyclonal antibody raised against 303–464 amino acids of GPC3 in their analysis. The specificity of their ELISA is to be confirmed because it is not sandwich ELISA, despite the many nonspecific bands the antibody detected in their immunoblotting. Moreover, the standard used in the assay was not recombinant GPC3 but a supernatant of HepG2 cells that is a mixture of many heterogeneous proteins. It is possible that they are measuring a mixture of nonspecific but HCC-related proteins. Capurro *et al.* (29) used a polyclonal antibody and a mAb, both raised against the last 70 amino acids of the COOH-terminal portion of GPC3, to detect glycanated GPC3 in serum with their sandwich ELISA. However, the major detectable form of GPC3 in serum is sGPC3, which cannot be detected with these antibodies against the COOH-terminal portion, as shown clearly in the present study. In fact, we examined many combinations of mAbs in our sandwich ELISA, but we could detect signal only when we used a combination of two N-mAbs (data not shown). Furthermore, the only evidence reported previously for the extracellular localization of glycanated GPC3 is immunoblotting of HepG2 cell culture supernatant, rather than serum from HCC patients. Here, we demonstrated that sGPC3 is in the culture supernatant and serum of the HCC patients using both immunoblotting and sandwich ELISA with the same combination of mAbs. One possible interpretation of the result, obtained by Capurro *et al.*, is that they are detecting some short fragments derived from a COOH-terminal portion but not the glycanated form of GPC3, and this issue should be further investigated.

We have delineated the usefulness of sGPC3 as highly sensitive to early-stage HCC. In addition, there were several cases with elevated serum sGPC3 among LC patients, although not included in this study, where HCC developed within 6 months after serum examination or some tumor was already detected by ultrasound without final diagnosis of HCC by computed tomography or angiography. We have also demonstrated the complementarity of sGPC3 to another HCC marker, AFP. These findings promise future bedside use of sGPC3 as a serological marker of HCC. Another attractive aspect of GPC3 is that the membrane-anchored portion is a potential target for antibody therapy. In this context, diagnosis with serum sGPC3 is useful not only in early detection of HCC but also for future identification of patients with high sGPC3 levels for tailor-made HCC therapy. Thus, further investigation into the clinical aspects of GPC3 in HCC is warranted.

ACKNOWLEDGMENTS

We thank H. Meguro and S. Fukui for excellent technical assistance and H. Satoh for providing pGEX-5X-sGPC3 construct.

REFERENCES

1. Befeler AS, Di Bisceglie AM. Hepatocellular carcinoma: diagnosis and treatment. Gastroenterology 2002;122:1609–19.

2. Gebo KA, Chander G, Jenckes MW, et al. Screening tests for hepatocellular carcinoma in patients with chronic hepatitis C: a systematic review. Hepatology 2002;36: S84–92.
3. Johnson PJ. The role of serum α-fetoprotein estimation in the diagnosis and management of hepatocellular carcinoma. Clin Liver Dis 2001;5:145–59.
4. Taketa K. α-Fetoprotein: reevaluation in hepatology. Hepatology 1990;12:1420–32.
5. Kanetaka K, Sakamoto M, Yamamoto Y, et al. Overexpression of tetraspanin CO-029 in hepatocellular carcinoma. J Hepatol 2001;35:637–42.
6. Kondoh N, Shuda M, Tanaka K, et al. Enhanced expression of S8, L12, L23a, L27 and L30 ribosomal protein mRNAs in human hepatocellular carcinoma. Anticancer Res 2001;21:2429–33.
7. Scuric Z, Stain SC, Anderson WF, Hwang JJ. New member of aldose reductase family proteins overexpressed in human hepatocellular carcinoma. Hepatology 1998; 27:943–50.
8. Tanaka K, Kondoh N, Shuda M, et al. Enhanced expression of mRNAs of antisecretory factor-1, gp96, DAD1 and CDC34 in human hepatocellular carcinomas. Biochim Biophys Acta 2001;1536:1–12.
9. Shirota Y, Kaneko S, Honda M, Kawai HF, Kobayashi K. Identification of differentially expressed genes in hepatocellular carcinoma with cDNA microarrays. Hepatology 2001;33:832–40.
10. Okabe H, Satoh S, Kato T, et al. Genome-wide analysis of gene expression in human hepatocellular carcinomas using cDNA microarray: identification of genes involved in viral carcinogenesis and tumor progression. Cancer Res 2001;61:2129–37.
11. Smith MW, Yue ZN, Geiss GK, et al. Identification of novel tumor markers in hepatitis C virus-associated hepatocellular carcinoma. Cancer Res 2003;63:859–64.
12. Xu XR, Huang J, Xu ZG, et al. Insight into hepatocellular carcinogenesis at transcriptome level by comparing gene expression profiles of hepatocellular carcinoma with those of corresponding noncancerous liver. Proc Natl Acad Sci USA 2001;98: 15089–94.
13. Chen X, Cheung ST, So S, et al. Gene expression patterns in human liver cancers. Mol Biol Cell 2002;13:1929–39.
14. Chuma M, Sakamoto M, Yamazaki K, et al. Expression profiling in multistage hepatocarcinogenesis: identification of HSP70 as a molecular marker of early hepatocellular carcinoma. Hepatology 2003;37:198–207.
15. Midorikawa Y, Ishikawa S, Iwanari H, et al. Glypican-3, overexpressed in hepatocellular carcinoma, modulates FGF2 and BMP-7 signaling. Int J Cancer 2003;103: 455–65.
16. Hsu HC, Cheng W, Lai PL. Cloning and expression of a developmentally regulated transcript MXR7 in hepatocellular carcinoma: biological significance and temporospatial distribution. Cancer Res 1997;57:5179–84.
17. Zhu ZW, Friess H, Wang L, et al. Enhanced glypican-3 expression differentiates the majority of hepatocellular carcinomas from benign hepatic disorders. Gut 2001;48: 558–64.
18. Zhou XP, Wang HY, Yang GS, et al. Cloning and expression of MXR7 gene in human HCC tissue. World J Gastroenterol 2000;6:57–60.
19. Mast AE, Higuchi DA, Huang ZF, et al. Glypican-3 is a binding protein on the HepG2 cell surface for tissue factor pathway inhibitor. Biochem J 1997;327:577–83.
20. Niwa H, Yamamura K, Miyazaki J. Efficient selection for high-expression transfectants with a novel eukaryotic vector. Gene (Amst.) 1991;108:193–9.
21. Filmus J, Church JG, Buick RN. Isolation of a cDNA corresponding to a developmentally regulated transcript in rat intestine. Mol Cell Biol 1988;8:4243–9.
22. Filmus J. Glypicans in growth control and cancer. Glycobiology 2001;11:19R–23R.
23. Pilia G, Hughes-Benzie RM, MacKenzie A, et al. Mutations in GPC3, a glypican gene, cause the Simpson-Golabi-Behmel overgrowth syndrome. Nat Genet 1996;12: 241–7.
24. Lin H, Huber R, Schlessinger D, Morin PJ. Frequent silencing of the GPC3 gene in ovarian cancer cell lines. Cancer Res 1999;59:807–10.
25. Xiang YY, Ladeda V, Filmus J. Glypican-3 expression is silenced in human breast cancer. Oncogene 2001;20:7408–12.
26. Kim H, Xu GL, Borczuk AC, et al. The heparan sulfate proteoglycan GPC3 is a potential lung tumor suppressor. Am J Respir Cell Mol Biol 2003;6:694–701.
27. Filmus J, Shi W, Wong ZM, Wong MJ. Identification of a new membrane-bound heparan sulphate proteoglycan. Biochem J 1995;311:561–5.
28. Nakatsura T, Yoshitake Y, Senju S, et al. Glypican-3, overexpressed specifically in human hepatocellular carcinoma, is a novel tumor marker. Biochem Biophys Res Commun 2003;306:16–25.
29. Capurro M, Wanless IR, Sherman M, et al. Glypican-3: a novel serum and histochemical marker for hepatocellular carcinoma. Gastroenterology 2003;125:89–97.